A unique cell division protein critical for the assembly of the bacterial divisome

Xiao Chu[1]*, Lidong Wang[1], Yiheng Zhu[1], Zhengshan Feng[1], Qingtian Guan[2], Lei Song[1]*, Zhaoqing Luo[1]*

[1]Department of Respiratory Medicine, Infectious Diseases and Pathogen Biology Center, State Key Laboratory for Diagnosis and Treatment of Severe Zoonotic Infectious Diseases, Key Laboratory for Zoonosis Research of the Ministry of Education, The First Hospital of Jilin University, Changchun, China

[2]Bioinformatics Laboratory, The First Hospital of Jilin University, Changchun, China

*Correspondence: chuxiao@jlu.edu.cn, lsong@jlu.edu.cn, and luoz@jlu.edu.cn

Abstract

Identification of unique essential bacterial genes is important for not only the understanding of their cell biology but also the development of new antimicrobials. Here we report a previously unrecognized core component of the *Acinetobacter baumannii* divisome. Our results reveal that the protein, termed Aeg1 interacts with multiple cell division proteins, including FtsN, which is required for components of the divisome to localize to the midcell. We demonstrate that the $FtsA_{E202K}$ and $FtsB_{E65A}$ mutants effectively bypassed the need of Aeg1 by *A*. *baumannii*, as did the activation variants $FtsW_{M254I}$ and $FtsW_{S274G}$. Our results suggest that Aeg1 is a cell division protein that arrives at the division site to initiate cell division by recruiting FtsN, which activates FtsQLB and FtsA to induce the septal peptidoglycan synthase FtsWI. The discovery of the new essential cell division protein has provided a new target for the development of antibacterial agents.

Keywords: conditional gene deletion; essential gene; cell division; antibacterial targets

Introduction

Acinetobacter baumannii is a Gram-negative bacterial pathogen that causes a wide variety of nosocomial infections (1, 2), including urinary tract infections, gastrointestinal and skin/wound infections and secondary meningitis (3-6). The challenge posed by this pathogen is compounded by the emergence of isolates that are resistant to almost all of the available antibiotics, including some of the last resort for treatment of infections caused by bacterial pathogens, including colistin, tigecycline, and carbapenems (2, 7). As a result, the World Health Organization (WHO) has classified *A. baumannii* as a pathogen for which new antibiotics are urgently needed (8). Meeting this challenge requires the discovery of antimicrobials of new mechanisms with action or other mitigation strategies that enable reduction of disease burden caused by this pathogen.

Historically, the discovery of antibiotics was largely based on the search for secondary metabolites produced by soil-dwelling microbes (9, 10). The majority of clinically used antibiotic classes originate from soil bacteria, including lactams, aminoglycosides, polymyxins, and glycopeptides (11). Unfortunately, natural products discovery is now plagued by problems of so-called ‘dereplication problem’, wherein rediscovery of molecules or their close relatives (12). As a result, there has not been a novel antibiotic discovered in over 30 years using traditional methods of screening environmental samples (13). The overuse of these merely variants of existing compounds has further accelerated the problem associated with antibiotic resistance. Thus, identification of novel therapeutic targets in the pathogen may serve as an effective alternative to the problem.

A better understanding of gene function associated with *A. baumannii* pathogenesis and biology will provide us strategies to develop antibiotics with potentially novel mechanisms of action. One extensively explored avenue in this regard is the identification of previously unrecognized essential genes by methods enabled by new DNA sequencing technologies, including insertion sequencing (INSeq) (14), transposon sequencing (Tn-seq) (15)， transposon-directed insertion site sequencing (TraDIS) (16), and high-throughput insertion tracking sequencing (HITS) (17). Application of these methods has identified genes believed to be required for bacterial viability under various conditions in such important pathogens as *Streptococcus pneumoniae* (15), *Pseudomonas aeruginosa* (18), *Vibrio cholerae* (19) and *A.*

baumannii (20-22).

Similar to candidate genes identified by other methods, putative essential genes obtained by In-seq were deduced from sequencing results of surviving mutants, some of which can be false positives or negatives due to unsaturated mutant libraries or polar effects on downstream genes of the insertion sites. Using In-seq Wang et al identified 453 candidate essential genes for the growth of *A. baumannii* strain ATCC 17978 on rich medium (22). Among these, genes annotated as hypotheticals with orthologs in other taxonomically distant microorganisms are of particular interest because their potential role in cellular processes that can be explored as targets for the development of novel antimicrobials. We thus set out to test a subgroup of the predicted essential genes by a conditional gene deletion strategy based on the arabinose inducible promoter (23). From ten genes examined, three were found to be essential for *A. baumannii* viability on rich medium. Further study revealed that one of these genes codes for a novel bacterial cell division protein.

Results

Identification of genes required for *A. baumannii* viability

Analysis of strains of *A. baumannii*, including the model strain 17978 by In-seq technologies have led to the identification of at least 453 genes potentially required for bacterial growth on rich medium (21, 22). Whereas many of these genes are involved in known cellular processes fundamental for cell viability such as DNA replication, transcription and translation, some code for proteins of unknown activity, are thus of great interest as potentially new antimicrobial targets (21). To determine the function of the candidate essential genes annotated as hypotheticals, we first confirmed their essentiality by a conditional gene deletion method. To this end, we employed a set of plasmids that allow inducible gene expression in *A. baumannii* (24). Each gene of interest was expressed from the arabinose-inducible promoter (23), and the corresponding gene was deleted from the chromosome by the standard allele exchange method (25) **(Fig. 1A)**. Chromosomal deletion mutants harboring the arabinose-inducible gene were tested for essentiality by spotting serially diluted cells onto solid medium with or without arabinose (ara) **(Fig. 1A)**. If the gene of interest is essential, the bacterium should fail to grow on plates without ara.

Our initial analysis of 10 genes (**Supplementary Files 1**) identified *A1S_0137*,

A1S_2249, and *A1S_3387* (26) that met the criteria of being required for growth on LB agar (**Fig. 1B**). Importantly, gene *A1S_3387* is also essential for *A. baumannii* growth in the Vogel-Bonner minimal medium with succinate (VBS) as the sole carbon source (27) **(Fig.1-figure supplement 1)**. These genes were thus designated as *A. baumannii* essential genes (Aeg) and Aeg1 (*A1S_3387*) was chosen for detailed study.

Sequence analysis revealed that Aeg1 has orthologs in a number of Gram-negative bacteria, including *Klebsiella pneumoniae*, *Salmonella enterica* members of the *Moraxellaceae* family and some strains of *Escherichia coli*, with sequence similarity ranging from 80% to identical **(Fig. 1-figure supplement 2).** Aeg1 is predicted to harbor a single transmembrane domain, however, the precise location of this transmembrane segment has been predicted differently across various analyses. SMART Web site (28) predicted the transmembrane region to be located at the N-terminus of Aeg1 (7-29 aa). In contrast, Phobius, based on HMM suggested the transmembrane segment is situated more centrally within the Aeg1 protein (134-151 aa), and further proposed that the N-terminus may correspond to a signal peptide (29, 30). Regardless of the specific transmembrane topology prediction, the N-terminal region of Aeg1 appears to be a critical domain. Therefore, to further elucidate the structural and functional importance of the Aeg1 close to its N-terminus end, we employed a dual inducible system with two compatible plasmids that use promoters that respond to ara and isopropyl-β-D-thiogalactopyranoside (IPTG), respectively. Strain Δ*aeg1*(P_{BAD}::Aeg1, P_{TAC}::Aeg1) was able to grow on medium containing 1% ara or 0.5 mM IPTG **(Fig. 1C)** indicating that the chromosomal deletion can be complemented by either of the constructs when expression of Aeg1 was induced. Importantly, expression of the Aeg1 mutant lacking N-terminal region was unable to restore the growth of the strain (**Fig. 1C**), suggesting that N-terminal domain of Aeg1 is essential for its activity.

Depletion of Aeg1 caused cell filamentation in *A. baumannii*.

We next examined the morphology of *A. baumannii* lacking Aeg1 by optical and scanning electron microscopy. Cultures of strain Δ*aeg1*(P_{BAD}::Aeg1) were induced by ara for 14 h, cells diluted into fresh LB with or without ara were allowed to grow for 18 h. We found that cells of cultures grown in medium containing 1% ara exhibited a short rod cell shape similar to that of the wild-type strain (**Fig. 2A**). In medium without ara most cells of strain

Δ*aeg1*(P_{BAD}::Aeg1) displayed an elongated morphology which is in sharp contrast to those of wild-type cells grew under identical conditions (**Fig. 2A**). Quantitative analysis indicated that in medium supplemented with ara, more than 95% of the cells of strain Δ*aeg1*(P_{BAD}::Aeg1) were shorter than 5 μm. Incubation in medium without ara for 18 h caused more than 96% of the cells to become elongated with cell lengths ranging from 5 μm to over 10 μm (**Fig. 2B**). The phenotype can be partially reversed after growing the elongated cells in medium containing 1% ara for 4 h (**Fig. 2C**). These results indicate that depletion of Aeg1 causes cell elongation, a phenotype that had been observed in recent studies using transposon insertion sequencing (20, 31).

Mutations in the cell division gene *ftsA* bypasses the requirement of Aeg1

To explore the cellular process participated by Aeg1, we sought to isolate suppressor mutants that can survive in standard medium under conditions the gene is not expressed. To this end, cells of strain Δ*aeg1*(P_{BAD}::Aeg1) grown in medium supplemented with ara were exposed to the mutagen ethyl methanesulfonate (EMS), and the treated cells were plated on LB agar without ara. A few colonies were obtained from approximately $6x10^8$ cells and two independent mutants M1 and M2 were chosen for further analysis. In spotting assays using diluted cells, each of these two mutants derived from strain Δ*aeg1*(P_{BAD}::Aeg1) was able to grow on medium without ara at rates comparable to those of wild-type bacteria (**Fig. 3A)**. We then performed whole genome sequencing analysis of these two mutants, which revealed that M1 and M2 had 320 and 328 substitution mutations, respectively. In addition, 659 insertion-deletion (InDel) mutations were found in M1 and 665 such mutations were associated with M2 **(Supplementary Files 2)**.

Because depletion of Aeg1 caused cell elongation, we first examined mutated genes whose functions are known to be involved in cell division. An E202K mutation caused by a G to A substitution in the first position of the codon was found in the cell division protein FtsA in both M1 and M2 (**Supplementary Files 2**). We thus verified the suppression phenotype by introducing a plasmid expressing FtsA or $FtsA_{E202K}$ into strain Δ*aeg1*(P_{BAD}::Aeg1) and examined the growth of the resulting bacterial strains under different induction conditions. Expression of $FtsA_{E202K}$ allowed strain Δ*aeg1*(P_{BAD}::Aeg1) to gain the ability to grow in the absence of ara. In contrast, although the protein was expressed at a comparable level, FtsA

cannot suppress the growth defect caused by Aeg1 depletion (**Fig. 3B**). Consistent with the growth phenotypes, expression of $FtsA_{E202K}$ in strain Δ*aeg1*(P_{BAD}::Aeg1) under conditions in which the complementation gene was not expressed displayed a morphology similar to that of wild-type bacteria (**Fig. 3C**).

Previous studies have found that several mutations in FtsA bypassed the requirement of a number of essential cell division proteins in *E. coli*, including ZipA (32), FtsK (33), and FtsN (34). Among these, $FtsA_{R286W}$ (FtsA*) was the first gain-of-function mutation found in *E. coli*, which allowed the survival of mutants lacking ZipA (Δ*zipA*) or FtsK (Δ*ftsK*) (32, 33, 35). Additionally, $FtsA_{I143L}$(36) and $FtsA_{E124A}$(34) weakly bypassed the requirement of FtsN. These mutations also rescued the $FtsL_{L86F/E87K}$ mutant when overexpressed (37). We thus examined whether similar mutations in FtsA of *A. baumannii* can bypass the need of Aeg1 by constructing substitution FtsA mutants D124A, V144L and Q285W, which correspond to E124A, I143L, and R286W in its *E. coli* counterpart, respectively (**Fig. 3-figure supplement 1**) and tested them in strain Δ*aeg1*(P_{BAD}::Aeg1). Whereas $FtsA_{Q285W}$ cannot detectably suppress Aeg1 depletion, expression of $FtsA_{D124A}$ or $FtsA_{V144L}$ partially resecured the growth of strain Δ*aeg1*(P_{BAD}::Aeg1) in medium without ara (**Fig. 3D**). Despite multiple attempts, we were unable to detect the expression of these FtsA mutants by immunoblotting using antibody specific to the Flag epitope fused to these alleles (**Fig. 3D, lower panels**), suggesting that the low activity exhibited by these mutants may result from low protein levels.

The observation that mutations in genes involved in cell division bypass the need of Aeg1 suggests that this protein participate in the same cellular process. We thus analyzed the cellular localization of Aeg1 in *A. baumannii* by introducing a plasmid that expresses Aeg1-mCherry from the P_{BAD} promoter. Fluorescence microscopy analysis revealed that Aeg1 localized at the septum of dividing cells (**Fig. 3E**), which validated the genetic evidence for its role in cell division.

Aeg1 interacts with multiple core components of the *A. baumannii* divisome

To further explore the possibility that Aeg1 is a component of the *A. baumannii* divisome, we determined its interactions with known cell division proteins using the Cya-based bacterial two-hybrid method (38). Effective complementation between the fused T25 and

T18 domains requires their localization to the cytoplasmic compartment. Because the predicted transmembrane topology of Aeg1 is not unequivocal, with one model suggesting an N-terminal transmembrane segment and another proposing a more centrally located membrane-spanning domain. To circumvent potential artifacts arising from the ambiguous topological models of Aeg1, we generated two distinct fusion constructs, tethering the T25 domain to either the N-terminus or C-terminus of the Aeg1 protein. We then assessed the complementation between these Aeg1-T25 fusions and the potential binding partners fused to the T18 domain to evaluate the interaction between Aeg1 and other Fts proteins. Among the tested proteins FtsZ, FtsA, ZipA, FtsK, FtsQ, FtsL, FtsB, FtsW, FtsI, and FtsN, Aeg1 detectably interacts with ZipA, FtsK, FtsL, FtsB, and FtsN. Intriguingly, ZipA and FtsN appearing to have higher binding affinity with Aeg1 whether the T25 reporter domain was fused to the N-terminus or C-terminus of the Aeg1 construct (**Fig. 4A-D**), as indicated by the hydrolysis of X-gal by derivatives of the *E. coli* reporter strain BTH101 (38) harboring appropriate protein fusions. When the interactions were quantitatively determined by measuring galactosidase activity, the binding of FtsN or ZipA to Aeg1 appeared the strongest among all examined protein pairs (**Fig. 4A-D**). This observation suggests that the precise topology of Aeg1 does not significantly impact its ability to engage these binding partners.

We next analyzed the localization of putative Aeg1-interacting proteins identified in our bacterial two-hybrid experiments. To this end, we coexpressed the mCherry-Aeg1 fusion with GFP fusion of ZipA, FtsL, FtsB, or FtsN in the WT strain from the ara- and IPTG-inducible promoter, respectively. Prior to localization studies, we first sought to examine the functionality of the GFP fusions by individually deleting the chromosomal gene of *zipA, ftsB*, *ftsL,* and *ftsN* in *A. baumannii* strains expressing the fusion proteins from a plasmid. Our results indicate that each GFP fusion was capable of complementing the growth defects caused by deleting the corresponding gene (**Fig. 4-figure supplement 1A**). Similarly, we found that expression of the mCherry-Aeg1 fusion allowed the deletion of the *aeg1* gene (**Fig. 4-figure supplement 1B**). In each case, the growth of the strain expressing the fusion protein complementing the chromosomal deletion was comparable to that of the wild-type strain (**Fig. 4-figure supplement 1A**). These strains were then used in experiments aiming at investigating the localization of the relevant proteins. Saturated

cultures of strains derived from WT(P_{BAD}::mCherry-Aeg1) (grown for 16 h) that harbored the GFP fusions were diluted into fresh LB broth. When the cell density of the subcultures reached OD_{600}=0.6, IPTG (0.25 mM) or ara (0.25%) were added to induce the expression of fusion proteins for 4 h and samples were processed for microscopic analysis. Consistent with results from the protein interaction experiments using the bacterial two-hybrid assay, we found that Aeg1 colocalized with ZipA, FtsL, FtsB, and FtsN **(Fig. 4E, red arrows)**, but occasional non-co-localization was also observed **(Fig. 4E, white arrows)**. Thus, Aeg1 interacts with multiple core cell divisome proteins of *A. baumannii*.

Aeg1 is an essential core cell division protein in *A. baumannii*

The interaction map between Aeg1 and core divisome proteins prompted us to postulate that the absence of Aeg1 prevented these proteins from localizing to the midcell. To test this hypothesis, we introduced plasmids that direct the expression of GFP fusion of each of the divisome proteins into strain Δ*aeg1*(P_{BAD}::mCherry-Aeg1). We evaluated the protein of Aeg1-mCherry at 2, 4, and 6 h after withdrawing arabinose and found that at the 2 h and 4 h time points mCherry-Aeg1 was still readily detectable (**Fig. 5-figure supplement 1**). Importantly, we found that removal of arabinose for 6 h rendered Aeg1-mCherry undetectable in approximately 90% of the cells. We thus used the 6 h inducer withdraw to examine the effects of Aeg1 depletion. In cells depleted of Aeg1, all of the examined core division proteins displayed midcell mistargeting, including ZipA, FtsB, FtsL, and FtsN (**Fig. 5A**). These results suggest that Aeg1 is a new member of cell division protein, which plays a role in positioning several other core proteins at the septum of *A. baumannii*.

During the formation of the divisome, FtsN was believed to be the last protein being recruited to the septum where it converts FtsQLB and FtsA into their active forms, which subsequently activate the septal peptidoglycan synthase FtsWI (36, 39). If the interaction between Aeg1 and FtsN is critical for the ability of the latter to switch on FtsQLB and FtsA, constitutively active mutants of FtsQLB or FtsA should suppress the need of Aeg1 for cell viability. To test this hypothesis, we expressed HA-$FtsB_{E65A}$ and HA-$FtsL_{Q70K}$ of *A. baumannii* (equivalent to mutants of their *E. coli* counterparts that allow the bypass of the requirement of FtsN) (**Fig. 5-figure supplement 2**) (36, 40) in strain Δ*aeg1*(P_{BAD}::Aeg1) on medium without ara. Although the expression of HA-$FtsB_{E65A}$ was not detectable with the HA-specific

antibody, induction of this mutant completely restored the growth of the Δ*aeg1* mutant in the absence of Aeg1 (**Fig. 5B**). In contrast, a similarly constructed plasmid that directs the expression of HA-FtsB$_{D68H}$ cannot bypass the requirement of Aeg1 under the same conditions (**Fig. 5B**). Similarly expressed HA-FtsL$_{Q70K}$ detectably rescued bacterial growth without Aeg1 at a level considerably lower than that of FtsB$_{E65A}$ (**Fig. 5C**). The low or undetectable activity exhibited by FtsL$_{Q70K}$ and FtsB$_{D68H}$ may result from the low protein levels in strain Δ*aeg1*(P$_{BAD}$::Aeg1). Nevertheless, these results support our hypothesis that Aeg1 functions upstream of FtsN, probably by functioning as its activator or recruiting factor.

It is known that expression of mutants FtsI$_{K211I}$, FtsW$_{M269I}$, and FtsW$_{E289G}$ driven by a strong promoter can bypass the need of FtsN in *E. coli* (41). The ability of FtsB$_{E65A}$ and FtsA$_{E202K}$ to suppress the growth defect of the Δ*aeg1* mutant prompted us to examine whether constitutively active alleles of FtsW or FtsI have the same effects. Overexpression of FtsW$_{M254I}$ and FtsW$_{S274G}$ of *A. baumannii* detectably rescued the growth of the strain in which Aeg1 had been depleted (**Fig. 5D**). FtsI from *A. baumannii* does not have a residue corresponding to K211 of its *E. coli* counterpart (**Fig. 5-figure supplement 2**), we thus did not test the effect of this mutation. Therefore, our results demonstrate that Aeg1 may collaborate with FtsN to activate at least a part of FtsQLB and FtsA for subsequently activation of FtsWI during cell division. Together with results that the variant FtsA$_{E202K}$ suppressed the growth defect caused by *aeg1* depletion (**Fig. 3B**), these observations support a model in which the Aeg1-FtsN complex is involved in the activation of FtsQLB and FtsA.

Discussion

Powerful In-seq DNA sequencing technologies based on saturated transposon insertion libraries have allowed the identification of genes essential for bacterial viability under specific conditions, including commonly used rich media such as LB broth (22). Using a conditional gene deletion method, we have revealed that from 10 putative essential genes identified by this method, three previously annotated as hypotheticals are essential for *A. baumannii* viability, suggesting that assignment of essentiality to genes identified by methods of this kind needs to be individually verified.

Our assignment of *aeg1* as an essential gene is consistent with a recent study which

revealed its essentiality (termed *advA*) by transposon insertion sequencing, which also observed cell elongation upon the depletion of this gene (31). Our results provided at least two additional lines of evidence to support the notion that Aeg1 is a core cell division protein in *A. baumannii*. First, random suppression mutations that bypassed the requirement of Aeg1 mapped to a classic cell division gene and mutations in some cell division genes known to circumvent the need of specific cell division proteins rescued the growth defect caused by Aeg1 depletion (**Fig. 3**). Second, Aeg1 interacts with at least a subset of proteins involved in cell division (**Fig. 4A-D**).

In the process of bacterial cell division, over 30 distinct proteins are assembled into a complex typically referred to as “divisome” (42). Ten of these are normally essential for both cell division and survival, and they are now mainly suggested to be the core of the divisome in various bacteria (42, 43). These essential division proteins are mostly named Fts (filamentation temperature sensitive), which stems from the fact that inactivating one of these *fts* genes causes cells to become filamentous, which eventually failed to survive (42, 44). Among these, the FtsQLB complex not only serves as a scaffold for recruitment of subsequent divisome proteins (45, 46), but also plays an important role in regulating the activity of the divisome (36, 39). The constriction control domain (CCD) of FtsL was previously defined as a critical component for switching the conformation of FtsLB from an off to an on state in order to activate FtsWI by enabling the interaction between $FtsI^{peri}$ and the AWI (activation of FtsWI) region of FtsL (36, 39, 47). Division obstruction caused by Aeg1 depletion can be effectively circumvented by suppression mutations ($FtsB_{E65A}$) in its CCD domain and by activation mutations (M254I and S274G) of FtsW **(Fig. 5D),** suggesting that Aeg1 functions upstream of these proteins.

In addition to FtsQLB-mediated activation of FtsI in the periplasm, the constitutively active form of FtsA (FtsA*) acting on FtsW in the cytoplasm, these two events functions synergistically to activate FtsWI for sPG synthesis (37). FtsA is a member of the actin family (48, 49), which interacts with FtsN via a unique IC domain positioned between the IA and IIA domains (50-52). Little is known about the function of the IA and IIA domains of FtsA. That the E202K mutation in the IIA domain bypasses the requirement of Aeg1 by *A. baumannii* **(Fig. 3B**) suggests that Aeg1 and FtsA work together to activate FtsW.

The maturation of the core divisome is facilitated by the recruitment in a nearly sequential order of the late-division proteins FtsK, FtsQ, FtsL/FtsB, FtsW, FtsI, and FtsN (53-55). Once the latest division protein, FtsN, is recruited, division-specific peptidoglycan synthesis conferred by the FtsWI complex is activated to build the septum (55, 56). More recent studies suggest that by binding to FtsA, a small amount of FtsN is recruited to the division site earlier than previously thought (36, 52, 57) where it induces a conformational switch in both FtsA and the FtsQLB subcomplex on both sides of the membrane (36). Furthermore, binding between FtsA and FtsN is regulated by ZipA (52). Our observation of strong binding of Aeg1 to ZipA and FtsN **(Fig. 4A-D)** prompted us to propose a model in which Aeg1 participates in cell division by anchoring to the division site together with ZipA where it recruits FtsN, which in turn signals to both the cytoplasmic or periplasmic branches of peptidoglycan synthesis involving FtsA and the FtsQLB complex, respectively (36) (**Fig. 6A**). The placement of Aeg1 as one of the early arrivals in the hierarchical sequential assembly of the divisome is consistent with the fact that the requirement of Aeg1 can be bypassed by constitutively active mutants of $FtsA_{E202K}$ (**Fig. 3**), FtsB ($FtsB_{E65A}$), FtsL ($FtsL_{Q70K}$) and of FtsW ($FtsW_{M254I}$ and $FtsW_{S274G}$) (**Fig. 5**).

It is worth noting that that although homologs of Aeg1 are present in many Gram-negative bacteria, including some recent isolate of *E. coli,* it appears to be absent in more extensively studied model strains such as K12 **(Figure 1-figure supplement 2).** It is possible that in strain K12, its activity is conferred by a yet unidentified protein that employs a conserved mechanism in cell division. Future study aiming at elucidating the biochemical and structural basis of the activity of Aeg1 and its homologs, and their relationship with other components of the divisome may provide not only insights into the mechanism of bacterial cell division but also leads for the design of antibiotics with novel mechanism of action.

Materials and methods

Bacterial strains, growth conditions, and plasmids construction

All bacterial strains and plasmids used in this study are listed in **Supplementary Files 3**. All *A. baumannii* strains were derivatives of strain ATCC17978 (58). Bacteria were grown in Luria Bertani (LB) broth or agar. Antibiotics were added to media when necessary. For *E. coli*,

the concentrations used were: ampicillin, 100 μg/mL, kanamycin, 30 μg/mL, chloramphenicol, 30 μg/mL, and gentamicin, 10 μg/mL. For *A. baumannii,* kanamycin, 30 μg/mL, gentamicin, 10 μg/mL, and streptomycin, 100 μg/mL.

To construct pUT18C-Flag, two oligos with sequences coding for the Flag tag and appropriate restriction sites were mixed at a 1: 1 ratio, heated to 100°C for 5 min and allowed the mixed DNA to anneal by gradually cooling down to room temperature. The resultant DNA fragment was then inserted into *Sal*I/*Cla*I digested pUT18C (38). We introduced an *Eco*RV site into the inserted DNA fragment to facilitate the identification of plasmids carrying the intended insert. To make pJL05 that allows P_{TAC}-driven expression of HA-tagged protein, primers containing the coding sequence of the HA tag were used to amplified the promoter region of pJL02 (24), PCR product was inserted as a *Pci*I/*BamH*I fragment. This manipulation replaced the Flag tag on pJL02 with an HA tag. pJL03 is a pVRL1-based plasmid harboring $P_{BAD,}$ which allows expressing Flag-tagged proteins in *A. baumannii* (24).

The DNA fragment were amplified from genomic DNA of *A. baumannii* strain and digested with appropriate restriction enzyme **(Supplementary Files 3)**, following insert into similarly digested plasmids. The experimental procedure entails fusion of the GFP gene with the target gene, followed by ligation of the resulting construct into the pJL05 vector for subsequent expression.

Introduction of plasmids into *A. baumannii*

Plasmids were introduced into *A. baumannii* by electroporation (59) or by triparental mating. Electrocompetent cells were prepared using a previously described protocol (60) with minor modifications. Briefly, saturated cultures of *A. baumannii* were diluted 1:100 into 50 mL LB medium to grow for 18 h at 37°C and cells were harvested by centrifugation (4000*g*) at room temperature (RT) for 5 min. Cells were washed twice with 10 mL of 10% glycerol, resuspended in 1 mL of 10% glycerol, cells aliquoted in 50 μL. were stored at -80˚C. For transformation, 1 μg of plasmid DNA was mixed with 50 μL competent cells and electroporation was performed in 0.2-cm cuvettes on a Bio-Rad Gene Pulser system (2.5 kV/cm, 25 μF, 200 Ω).

The *E. coli* MT607 harboring pRK600 (61) was used for triparental mating. Briefly, 100

362 μL of overnight cultures of the donor, recipient, and the helper strain were mixed and cells
363 were harvest by centrifugation (4000*g*) for 5 min. Mixed cells washed twice with 1 mL of
364 sterile water were spotted onto LB agar and the mating was allowed to proceeded for 4-6 h
365 at 37°C before plating onto selective medium.

366 **Construction of in-frame deletion mutants of *A. baumannii***

367 To delete the putative essential genes, we first introduced a plasmid expressing the
368 gene of interest into *A. baumannii* and the resulting strains were used to construct
369 chromosomal deletion mutants using a method based on the suicide plasmid pSR47s (25).
370 Briefly, the coding region of the gene was inserted into pJL03, which allows expression of
371 Flag-tagged protein from the P_{BAD} promoter (24) and the resulting plasmid was introduced
372 into *A. baumannii* by electroporation. Strains in which the chromosomal deletion is
373 complemented by GFP or mCherry fusions of the relevant Fts proteins were similarly
374 constructed.

375 To construct the plasmid used for in-frame deletion of *A. baumannii* genes, 1.0 kilobase
376 DNA fragment was amplified from the upstream and downstream of the gene to delete,
377 respectively, digested with appropriate restriction enzymes and inserted into similarly
378 digested pSR47s (25). The primers were designed so that in each case the gene to be
379 deleted was replaced with an open reading frame consisting of the first and last 15 residues
380 linked by two amino acids encoded by the sequence of the restriction enzyme used to fuse
381 the two DNA fragments (**Supplementary Files 3**). The plasmid was then introduced into the
382 *A. baumannii* strain harboring the pJL03 derivative expressing the gene to be deleted from
383 the P_{BAD} promoter by triparental mating. Transconjugants obtained on LB agar containing
384 1% ara were grown in LB broth containing 5% sucrose for 18 h prior to being streaked onto
385 LB agar supplemented with 5% sucrose. Deletion mutants were identified by colony PCR
386 with primers corresponding to the 5' end of the upstream fragment and the 3' of the
387 downstream fragments.

388 **Ethyl methanesulfonate (EMS) mutagenesis**

389 The *A. baumannii* strain Δ*aeg1*(P_{BAD}::Aeg1) was grown in LB broth containing 1% ara to
390 saturation, cells from 2-mL culture collected by centrifugation were washed twice with cold
391 buffer A [60 mM K_2HPO_4, 33 mM KH_2PO_4, 7.6 mM $(NH_4)_2SO_4$, 1.7 mM sodium citrate, PH=7].

Cells resuspended in 2x buffer A supplemented with 1.4% EMS were incubated in a shaker (220 rpm) at 37°C for 15 min for 30 min, 45 min and 60 min, respectively. Treated cells harvested by centrifugation were washed twice with buffer A prior to being plated onto LB agar supplemented with 5% glucose. Colonies appeared were purified and tested by spotting diluted cells onto LB agar with or without ara, respectively to confirm the ability to grown in the absence Aeg1. To eliminate the possibility that the ara-independent growth phenotype was due to mutations in the P_{BAD} promoter, the plasmid from each mutant candidate was rescued and the promoter region was sequenced. Only mutants harboring an intact P_{BAD} promoter were retained for further study.

Genome sequencing was performed by Suzhou Golden Wisdom Biological Technology Co., Ltd, and mutations were identified using the genome of the parent strain ATCC 17978 as reference (26).

Bacterial Two-Hybrid assays

To assess interactions between Aeg1 and *A. baumannii* Fts proteins, we employed the *Bordetella pertussis* adenylate cyclase (Cya)-based bacterial two-hybrid system (38). The coding region of Aeg1 was fused to the T25 fragment of Cya and testing Fts proteins were individually fused to the T18 fragment on pUT18C-Flag, which allows the detection of the fusion protein with the Flag-specific antibody (**Supplementary Files 3**). Interaction was evaluated in the cya^- *E. coli* strain BTH101 (38) by the ability of the testing strains to hydrolyze X-Gal. Quantitative measurement of β-galactosidase activity with performed with ortho-nitrophenyl-β-galactoside (ONPG) using an established protocol (62). Testing bacterial strains were cultured in 2 mL LB broth containing 0.5 mM IPTG for 18 h, and 0.2 mL cells were harvest and resuspended in 1 mL Z-buffer (60 mM Na_2HPO_4, 40 mM $NaH_2PO_4 \cdot H_2O$, 1 mM $MgSO_4$, 10 mM KCl, and 7 mL of 2-mercaptoethanol per liter). After adding 50 μL 1% (m/v) SDS and 100 μL of chloroform, cells were lysed by 30 s vortex and 50 μL of ONPG (40 mg/mL) was added. The reaction was terminated with 500 μL of 1 M Na_2CO_3 after ONPG hydrolysis had occurred as determined the presence of the yellow color product. β-galactosidase activity is defined as in Miller units using the following equation: (OD_{420}×1000)/ [(time of incubation in min)x(volume of cell suspension in mL)x(cell density of

the culture in OD_{600})]. All assays were done in triplicate.

Antibodies and immunoblotting

HA-specific antibody (1:1000) was purchased from Santa Cruz (Cat #sc-7392), and rabbit anti-ICDH (1:2000) was described previously (24). To prepare protein samples, we diluted (1:100) saturated bacterial cultures into fresh LB broth. When OD_{600} of the cultures reached 0.6, IPTG was added to a final concentration of 0.5 mM. Approximately $1x10^9$ cells were collected, resuspended in 100 μL SDS sample buffer and were boiled for 5 min. Proteins separated by SDS-PAGE were transferred onto nitrocellulose membranes, which were first blocked with 5% nonfat milk for 1 h followed by incubation with appropriate primary antibodies for 14 h. Washed membranes were incubated with the appropriate IRDye-labeled secondary antibodies and signals were detected using an Odyssey CLx system (LI-COR).

Fluorescence imaging

To determine the cellular localization of Aeg1 and its colocalization with members of the divisome, we constructed pJL03::Aeg1-mCherry, which expressed the fusion from the P_{BAD} promoter (23). GFP chimera of Fts proteins were expressed from pJL05 driven by the P_{TAC} promoter inducible by IPTG. Each of the GFP-Fts fusion was introduced into strain WT(P_{BAD}::mCherry-Aeg1).

To visualize the localization of the fusions, bacterial strains were grown to saturation in LB broth containing ara and the cells washed twice with PBS were diluted to a density of approximately $5x10^6$ cells/mL. The cultures were split into two 2-mL subcultures, the one used to determine how the absence of Aeg1 impacted the cellular localization of Fts proteins received only IPTG but not ara. Cultures were incubated in a shaker for an additional 6 h, and 100 μL cells were withdrawn and fixed by incubation in glutaraldehyde for 20 min at RT. After washing twice with PBS, samples were stained with Hoechst 33342 (1:5000) (Invitrogen, cat#H3570) and mounted on slides for observation with an Olympus IX-83 fluorescence microscope.

Bioinformatics analysis

Aeg1 homologs were identified using tBLASTn (63) using the Aeg1 protein (*A1S_3387*) from strain ATCC17978 (GenBank: CP000521.1) as the query sequence. Clustal omega (https://www.ebi.ac.uk/Tools/msa/clustalo/) was used to perform multiple sequence

alignments. The homology comparison of Fts proteins between *E. coli* and *A. baumannii* was also performed using Clustal omega. Jalview was used for editing and viewing sequence alignments (64). The transmembrane regions of Aeg1 were predicted by the SMART Web sites (28) and Phobius web server (29, 30).

Data quantitation, statistical analyses

Student's *t*-test was used to compare the mean between two groups each with at least three independent samples.

Acknowledgements

This work in part was supported by the Natural Science Foundation of Jilin Province grant YDZJ202201ZYTS025 (XC), Jilin Science and Technology Agency grant 20200403117SF (LS), Science and Technology Development Project of Changchun City 23YQ10 (LS), and The Bethune Project of Jilin University 2024B20 (LS).

.

References

1. Wong D, Nielsen TB, Bonomo RA, Pantapalangkoor P, Luna B, Spellberg B. Clinical and Pathophysiological Overview of Acinetobacter Infections: a Century of Challenges. *Clinical microbiology reviews*. 2017;30:409-47.doi: 10.1128/cmr.00058-16
2. Piperaki ET, Tzouvelekis LS, Miriagou V, Daikos GL. Carbapenem-resistant Acinetobacter baumannii: in pursuit of an effective treatment. *Clinical microbiology and infection : the official publication of the European Society of Clinical Microbiology and Infectious Diseases*. 2019;25:951-7.doi: 10.1016/j.cmi.2019.03.014
3. Peleg AY, Seifert H, Paterson DL. Acinetobacter baumannii: emergence of a successful pathogen. *Clinical microbiology reviews*. 2008;21:538-82.doi: 10.1128/cmr.00058-07
4. Wroblewska MM, Towner KJ, Marchel H, Luczak M. Emergence and spread of carbapenem-resistant strains of Acinetobacter baumannii in a tertiary-care hospital in Poland. *Clinical microbiology and infection : the official publication of the European Society of Clinical Microbiology and Infectious Diseases*. 2007;13:490-6.doi: 10.1111/j.1469-0691.2007.01694.x
5. Nasr P. Genetics, epidemiology, and clinical manifestations of multidrug-resistant Acinetobacter baumannii. *The Journal of hospital infection*. 2020;104:4-11.doi: 10.1016/j.jhin.2019.09.021
6. Doi Y, Murray GL, Peleg AY. Acinetobacter baumannii: evolution of antimicrobial resistance-treatment options. *Seminars in respiratory and critical care medicine*. 2015;36:85-98.doi: 10.1055/s-0034-1398388
7. Karakonstantis S. A systematic review of implications, mechanisms, and stability of in vivo emergent resistance to colistin and tigecycline in Acinetobacter baumannii. *Journal of chemotherapy (Florence, Italy)*. 2021;33:1-11.doi: 10.1080/1120009x.2020.1794393
8. Whiteway C, Breine A, Philippe C, Van der Henst C. Acinetobacter baumannii. *Trends in microbiology*. 2022;30:199-200.doi: 10.1016/j.tim.2021.11.008
9. Clardy J, Fischbach MA, Walsh CT. New antibiotics from bacterial natural products. *Nature biotechnology*. 2006;24:1541-50.doi: 10.1038/nbt1266
10. Wright GD. Opportunities for natural products in 21(st) century antibiotic discovery. *Natural product reports*. 2017;34:694-701.doi: 10.1039/c7np00019g
11. Hutchings MI, Truman AW, Wilkinson B. Antibiotics: past, present and future. *Current opinion in microbiology*. 2019;51:72-80.doi: 10.1016/j.mib.2019.10.008
12. Cox G, Sieron A, King AM, De Pascale G, Pawlowski AC, Koteva K, et al. A Common Platform for Antibiotic Dereplication and Adjuvant Discovery. *Cell chemical biology*. 2017;24:98-109.doi: 10.1016/j.chembiol.2016.11.011
13. Lewis K. The Science of Antibiotic Discovery. *Cell*. 2020;181:29-45.doi: 10.1016/j.cell.2020.02.056
14. Goodman AL, McNulty NP, Zhao Y, Leip D, Mitra RD, Lozupone CA, et al. Identifying genetic determinants needed to establish a human gut symbiont in its habitat. *Cell host & microbe*. 2009;6:279-89.doi: 10.1016/j.chom.2009.08.003
15. van Opijnen T, Bodi KL, Camilli A. Tn-seq: high-throughput parallel sequencing for fitness and genetic interaction studies in microorganisms. *Nature methods*. 2009;6:767-72.doi: 10.1038/nmeth.1377
16. Langridge GC, Phan MD, Turner DJ, Perkins TT, Parts L, Haase J, et al. Simultaneous

assay of every Salmonella Typhi gene using one million transposon mutants. *Genome research*. 2009;19:2308-16.doi: 10.1101/gr.097097.109
17. Gawronski JD, Wong SM, Giannoukos G, Ward DV, Akerley BJ. Tracking insertion mutants within libraries by deep sequencing and a genome-wide screen for Haemophilus genes required in the lung. *Proceedings of the National Academy of Sciences of the United States of America*. 2009;106:16422-7.doi: 10.1073/pnas.0906627106
18. Gallagher LA, Shendure J, Manoil C. Genome-scale identification of resistance functions in Pseudomonas aeruginosa using Tn-seq. *mBio*. 2011;2:e00315-10.doi: 10.1128/mBio.00315-10
19. Dong TG, Ho BT, Yoder-Himes DR, Mekalanos JJ. Identification of T6SS-dependent effector and immunity proteins by Tn-seq in Vibrio cholerae. *Proceedings of the National Academy of Sciences of the United States of America*. 2013;110:2623-8.doi: 10.1073/pnas.1222783110
20. Bai J, Dai Y, Farinha A, Tang AY, Syal S, Vargas-Cuebas G, et al. Essential Gene Analysis in Acinetobacter baumannii by High-Density Transposon Mutagenesis and CRISPR Interference. *Journal of bacteriology*. 2021;203:e0056520.doi: 10.1128/jb.00565-20
21. Gallagher LA, Ramage E, Weiss EJ, Radey M, Hayden HS, Held KG, et al. Resources for Genetic and Genomic Analysis of Emerging Pathogen Acinetobacter baumannii. *Journal of bacteriology*. 2015;197:2027-35.doi: 10.1128/jb.00131-15
22. Wang N, Ozer EA, Mandel MJ, Hauser AR. Genome-wide identification of Acinetobacter baumannii genes necessary for persistence in the lung. *mBio*. 2014;5:e01163-14.doi: 10.1128/mBio.01163-14
23. Guzman LM, Belin D, Carson MJ, Beckwith J. Tight regulation, modulation, and high-level expression by vectors containing the arabinose PBAD promoter. *Journal of bacteriology*. 1995;177:4121-30.doi: 10.1128/jb.177.14.4121-4130.1995
24. Jie J, Chu X, Li D, Luo Z. A set of shuttle plasmids for gene expression in Acinetobacter baumannii. *PloS one*. 2021;16:e0246918.doi: 10.1371/journal.pone.0246918
25. Merriam JJ, Mathur R, Maxfield-Boumil R, Isberg RR. Analysis of the Legionella pneumophila fliI gene: intracellular growth of a defined mutant defective for flagellum biosynthesis. *Infection and immunity*. 1997;65:2497-501.doi: 10.1128/iai.65.6.2497-2501.1997
26. Smith MG, Gianoulis TA, Pukatzki S, Mekalanos JJ, Ornston LN, Gerstein M, et al. New insights into Acinetobacter baumannii pathogenesis revealed by high-density pyrosequencing and transposon mutagenesis. *Genes & development*. 2007;21:601-14.doi: 10.1101/gad.1510307
27. Vogel HJ, Bonner DM. Acetylornithinase of Escherichia coli: partial purification and some properties. *The Journal of biological chemistry*. 1956;218:97-106.doi:
28. Letunic I, Khedkar S, Bork P. SMART: recent updates, new developments and status in 2020. *Nucleic acids research*. 2021;49:D458-d60.doi: 10.1093/nar/gkaa937
29. Käll L, Krogh A, Sonnhammer EL. A combined transmembrane topology and signal peptide prediction method. *Journal of molecular biology*. 2004;338:1027-36.doi: 10.1016/j.jmb.2004.03.016
30. Käll L, Krogh A, Sonnhammer EL. Advantages of combined transmembrane topology and signal peptide prediction--the Phobius web server. *Nucleic acids research*.

2007;35:W429-32.doi: 10.1093/nar/gkm256
31. Geisinger E, Mortman NJ, Dai Y, Cokol M, Syal S, Farinha A, et al. Antibiotic susceptibility signatures identify potential antimicrobial targets in the Acinetobacter baumannii cell envelope. *Nature communications*. 2020;11:4522.doi: 10.1038/s41467-020-18301-2
32. Pichoff S, Shen B, Sullivan B, Lutkenhaus J. FtsA mutants impaired for self-interaction bypass ZipA suggesting a model in which FtsA's self-interaction competes with its ability to recruit downstream division proteins. *Molecular microbiology*. 2012;83:151-67.doi: 10.1111/j.1365-2958.2011.07923.x
33. Berezuk AM, Roach EJ, Seidel L, Lo RY, Khursigara CM. FtsA G50E mutant suppresses the essential requirement for FtsK during bacterial cell division in Escherichia coli. *Canadian journal of microbiology*. 2020;66:313-27.doi: 10.1139/cjm-2019-0493
34. Bernard CS, Sadasivam M, Shiomi D, Margolin W. An altered FtsA can compensate for the loss of essential cell division protein FtsN in Escherichia coli. *Molecular microbiology*. 2007;64:1289-305.doi: 10.1111/j.1365-2958.2007.05738.x
35. Geissler B, Elraheb D, Margolin W. A gain-of-function mutation in ftsA bypasses the requirement for the essential cell division gene zipA in Escherichia coli. *Proceedings of the National Academy of Sciences of the United States of America*. 2003;100:4197-202.doi: 10.1073/pnas.0635003100
36. Liu B, Persons L, Lee L, de Boer PA. Roles for both FtsA and the FtsBLQ subcomplex in FtsN-stimulated cell constriction in Escherichia coli. *Molecular microbiology*. 2015;95:945-70.doi: 10.1111/mmi.12906
37. Park KT, Pichoff S, Du S, Lutkenhaus J. FtsA acts through FtsW to promote cell wall synthesis during cell division in Escherichia coli. *Proceedings of the National Academy of Sciences of the United States of America*. 2021;118.doi: 10.1073/pnas.2107210118
38. Karimova G, Pidoux J, Ullmann A, Ladant D. A bacterial two-hybrid system based on a reconstituted signal transduction pathway. *Proceedings of the National Academy of Sciences of the United States of America*. 1998;95:5752-6.doi: 10.1073/pnas.95.10.5752
39. Tsang MJ, Bernhardt TG. A role for the FtsQLB complex in cytokinetic ring activation revealed by an ftsL allele that accelerates division. *Molecular microbiology*. 2015;95:925-44.doi: 10.1111/mmi.12905
40. Park KT, Du S, Lutkenhaus J. Essential Role for FtsL in Activation of Septal Peptidoglycan Synthesis. *mBio*. 2020;11.doi: 10.1128/mBio.03012-20
41. Li Y, Gong H, Zhan R, Ouyang S, Park KT, Lutkenhaus J, et al. Genetic analysis of the septal peptidoglycan synthase FtsWI complex supports a conserved activation mechanism for SEDS-bPBP complexes. *PLoS genetics*. 2021;17:e1009366.doi: 10.1371/journal.pgen.1009366
42. de Boer PA. Advances in understanding E. coli cell fission. *Current opinion in microbiology*. 2010;13:730-7.doi: 10.1016/j.mib.2010.09.015
43. Haeusser DP, Margolin W. Splitsville: structural and functional insights into the dynamic bacterial Z ring. *Nature reviews Microbiology*. 2016;14:305-19.doi: 10.1038/nrmicro.2016.26
44. Lutkenhaus J, Du S. E. coli Cell Cycle Machinery. *Sub-cellular biochemistry*. 2017;84:27-65.doi: 10.1007/978-3-319-53047-5_2
45. Carson MJ, Barondess J, Beckwith J. The FtsQ protein of Escherichia coli: membrane

topology, abundance, and cell division phenotypes due to overproduction and insertion mutations. *Journal of bacteriology*. 1991;173:2187-95.doi: 10.1128/jb.173.7.2187-2195.1991
46. Guzman LM, Weiss DS, Beckwith J. Domain-swapping analysis of FtsI, FtsL, and FtsQ, bitopic membrane proteins essential for cell division in Escherichia coli. *Journal of bacteriology*. 1997;179:5094-103.doi: 10.1128/jb.179.16.5094-5103.1997
47. Craven SJ, Condon SGF, Senes A. A model of the interactions between the FtsQLB and the FtsWI peptidoglycan synthase complex in bacterial cell division. 2022:2022.10.30.514410.doi: 10.1101/2022.10.30.514410 %J bioRxiv
48. Sánchez M, Valencia A, Ferrándiz MJ, Sander C, Vicente M. Correlation between the structure and biochemical activities of FtsA, an essential cell division protein of the actin family. *The EMBO journal*. 1994;13:4919-25.doi: 10.1002/j.1460-2075.1994.tb06819.x
49. van den Ent F, Löwe J. Crystal structure of the cell division protein FtsA from Thermotoga maritima. *The EMBO journal*. 2000;19:5300-7.doi: 10.1093/emboj/19.20.5300
50. Szwedziak P, Wang Q, Freund SM, Löwe J. FtsA forms actin-like protofilaments. *The EMBO journal*. 2012;31:2249-60.doi: 10.1038/emboj.2012.76
51. Baranova N, Radler P, Hernández-Rocamora VM, Alfonso C, López-Pelegrín M, Rivas G, et al. Diffusion and capture permits dynamic coupling between treadmilling FtsZ filaments and cell division proteins. *Nature microbiology*. 2020;5:407-17.doi: 10.1038/s41564-019-0657-5
52. Pichoff S, Du S, Lutkenhaus J. The bypass of ZipA by overexpression of FtsN requires a previously unknown conserved FtsN motif essential for FtsA-FtsN interaction supporting a model in which FtsA monomers recruit late cell division proteins to the Z ring. *Molecular microbiology*. 2015;95:971-87.doi: 10.1111/mmi.12907
53. Goehring NW, Beckwith J. Diverse paths to midcell: assembly of the bacterial cell division machinery. *Current biology : CB*. 2005;15:R514-26.doi: 10.1016/j.cub.2005.06.038
54. Du S, Henke W, Pichoff S, Lutkenhaus J. How FtsEX localizes to the Z ring and interacts with FtsA to regulate cell division. *Molecular microbiology*. 2019;112:881-95.doi: 10.1111/mmi.14324
55. Addinall SG, Cao C, Lutkenhaus J. FtsN, a late recruit to the septum in Escherichia coli. *Molecular microbiology*. 1997;25:303-9.doi: 10.1046/j.1365-2958.1997.4641833.x
56. Lyu Z, Yahashiri A, Yang X, McCausland JW, Kaus GM, McQuillen R, et al. FtsN maintains active septal cell wall synthesis by forming a processive complex with the septum-specific peptidoglycan synthases in E. coli. *Nature communications*. 2022;13:5751.doi: 10.1038/s41467-022-33404-8
57. Weiss DS. Last but not least: new insights into how FtsN triggers constriction during Escherichia coli cell division. *Molecular microbiology*. 2015;95:903-9.doi: 10.1111/mmi.12925
58. Piechaud M, Second L. [Studies of 26 strains of Moraxella Iwoffi]. *Annales de l'Institut Pasteur*. 1951;80:97-9.doi:
59. Fiedler S, Wirth R. Transformation of bacteria with plasmid DNA by electroporation. *Analytical biochemistry*. 1988;170:38-44.doi: 10.1016/0003-2697(88)90086-3
60. Yildirim S, Thompson MG, Jacobs AC, Zurawski DV, Kirkup BC. Evaluation of Parameters for High Efficiency Transformation of Acinetobacter baumannii. *Scientific reports*. 2016;6:22110.doi: 10.1038/srep22110

61. Finan TM, Kunkel B, De Vos GF, Signer ER. Second symbiotic megaplasmid in Rhizobium meliloti carrying exopolysaccharide and thiamine synthesis genes. *Journal of bacteriology*. 1986;167:66-72.doi: 10.1128/jb.167.1.66-72.1986
62. Miller JHJEimg. Assay of β-galactosidase. 1972.doi:
63. Gertz EM, Yu YK, Agarwala R, Schäffer AA, Altschul SF. Composition-based statistics and translated nucleotide searches: improving the TBLASTN module of BLAST. *BMC biology*. 2006;4:41.doi: 10.1186/1741-7007-4-41
64. Waterhouse AM, Procter JB, Martin DM, Clamp M, Barton GJ. Jalview Version 2--a multiple sequence alignment editor and analysis workbench. *Bioinformatics (Oxford, England)*. 2009;25:1189-91.doi: 10.1093/bioinformatics/btp033
65. Busiek KK, Margolin W. A role for FtsA in SPOR-independent localization of the essential Escherichia coli cell division protein FtsN. *Molecular microbiology*. 2014;92:1212-26.doi: 10.1111/mmi.12623

Fig. 1 Identification of *aeg1* as an essential gene for *A. baumannii* viability on rich medium

A. A diagram depicting the method for conditional deletion of potential essential genes. The gene to be examined was expressed from the arabinose-inducible promoter on a plasmid and the gene was deleted from the chromosome using the standard allele exchange method (upper panel) and strains lacking the chromosomal gene were tested for essentiality by spotting diluted cells on media with and without arabinose, respectively (lower panel).

B. Identification of *A1S_0137*, *A1S_2249,* and *A1S_3387* as *A. baumannii* essential genes*.* Each of the 10 genes predicted to be essential were deleted by the method described in A and the resulting bacterial strains were tested for growth by spotting serially diluted cells on medium with or without 1% arabinose. Images were acquired after incubation at 37°C for 18 h. Similar results were obtained in at least three independent experiments.

C. Cells harboring differentially regulated HA-Aeg1 and HA-Aeg1$^{\Delta N}$ spotted onto LB agar supplemented with 0.5 mM IPTG or 1% ara, images were acquired after 18 h incubation at 37°C **(C upper two panels)**. The expression of the Aeg1 and Aeg1$^{\Delta N}$ were examined by immunoblotting with the HA-specific antibody. The metabolic enzyme isocitrate dehydrogenase (ICDH) was probed as a loading control **(C, lower two panels)**. Similar results were obtained in three independent experiments.

Fig. 2 Aeg1 deficiency causes cell elongation in *A. baumannii*.

A. Cell morphology of the wild-type and strain Δ*aeg1*(P_{BAD}::Aeg1) grown in medium with or without ara. The Δ*aeg1*(P_{BAD}::Aeg1) and the wild-type strains were grown in medium with or without ara for 18 h, samples were processed for scanning electron microscope imaging. Images shown are representative of three parallel cultures. Bar, 2 µm.

B-C. Expression of Aeg1 reversed the cell elongation phenotype caused by its depletion. Saturated bacterial cultures of Δ*aeg1*(P_{BAD}::Aeg1) diluted in fresh LB broth with (I) or without (II) ara were incubated for 18 h. The culture from the uninduced sample was split into two subcultures, ara was added to one of the subcultures and the morphology of the cells was determined at 4 h (III) post induction. Images are representative of three parallel cultures. Bar, 10 µm **(B)**. Quantitation of the cell length in samples differently expressing Aeg1. Cell

length was categorized into groups of 0-5 μm, 5-10 μm, and more than 10 μm. At least 300 cells were counted for each sample **(C)**. Results shown were from the average of three independent experiments. Statistical analysis in each panel was performed by Student's *t* test.

Fig. 3 Mutations in proteins involved in cell division bypass the requirement of Aeg1.

A. Isolation of two suppressor mutants that gained viability in the absence of Aeg1. Cells serially diluted with water were spotted onto LB agar with or without ara. Note that the Δ*aeg1*(P_{BAD}::Aeg1) strain (top row) cannot grow on medium without ara and the wild-type strain (2nd row) can grow on both conditions. Similar results were obtained in three independent experiments.

B. The $FtsA_{E202K}$ mutant suppressed the requirement of Aeg1. Cells of strains derived from Δ*aeg1*(P_{BAD}::*aeg1*) that harbored the vector (I), pHA-Aeg1 (II), pHA-FtsA (III), or pHA-$FtsA_{E202K}$ (IV) were spotted onto LB agar containing ara (left) or IPTG (right), Images were acquired after 18 h incubation at 37°C **(b, upper panels)**. Expression of Aeg1, FtsA or $FtsA_{E202K}$ in these strains were detected by immunoblotting with the HA-specific antibody after lysates of IPTG-induced cells being resolved by SDS-PAGE. ICDH was probed as a loading control **(b, lower panels)**. Similar results were obtained in three independent experiments.

C. The suppression mutants assumed normal cell morphology. Bacterial strains derived from Δ*aeg1*(P_{BAD}::*aeg1*) grown in LB broth containing ara for 6 h were diluted into fresh medium with the inducer and the cultures were induced with IPTG for 4 h prior to being processed for imaging. Images were representatives of three parallel cultures. Bar, 10 μm.

D. Additional FtsA mutants bypassed the need of Aeg1. Mutant $FtsA_{D124A}$, $FtsA_{V144A}$, or $FtsA_{Q285A}$ expressed from the IPTG-inducible P_{TAC} was introduced into strain Δ*aeg1*(P_{BAD}::Aeg1) and serially diluted cells of resulting strains were spotted onto LB agar supplemented with ara or IPTG. Images were acquired after incubation at 37°C for 18 h **(upper panels)**. Expression of Aeg1, $FtsA_{D124A}$, $FtsA_{V144A}$, and $FtsA_{Q285A}$ in these strains. Total protein of IPTG-induced cells resolved by SDS-PAGE and proteins transferred onto nitrocellulose membranes were detected by immunoblotting with the HA-specific antibody.

ICDH was probed as a loading control **(lower panels).** Similar results were obtained in three independent experiments.

E. The Aeg1-mCherry fusion localizes to division constrictions. Wild-type *A. baumannii* harboring P_{BAD}::Aeg1-mCherry grown to the mid-log phase in LB broth containing 1% ara were processed for imaging. Bar, 10 µm. Images are representative of three parallel cultures.

Fig. 4 Aeg1 interacts with multiple core proteins of the *A. baumannii* divisome.

A-D. Derivatives of strain *E. coli* BTH101 containing T18-Aeg1 and T25 fusion of the indicated proteins were spotted onto LB agar containing X-gal. T25 domain was fused to the N-terminus **(A-B)** or C-terminus **(C-D)** of Aeg1. Images were acquired after incubation for 18 h at 37°C **(A and C)**. Interactions determined by quantitative measurement of β-galactosidase activity **(B and D)**. Results shown were from three independent experiments. Statistical analysis was performed by Student's *t* test.

E. Aeg1 colocalized with a set of core divisome proteins. GFP fusion of ZipA, FtsL, FtsB, or FtsN was expressed in strain WT(pJL03::mCherry-Aeg1). Saturated cultures of bacterial strains harboring the GFP and mCherry fusions were diluted into fresh LB broth. After the cell density of the subcultures reached until $OD_{600=}$0.6, IPTG (0.25 mM) and ara (0.25%) were added to induce the expression of fusion proteins for 4 h prior to being processed for imaging. Red arrows indicate the sites of colocalization. Cells in which the proteins did not co-localize were shown by white arrows. Bar, 10 µm. Images are representative of three independent cultures.

Fig. 5 Aeg1 dictates the cellular localization of core divisome proteins.

A. Aeg1 deficiency prevented core divisome proteins from localizing to the middle cell. Cells of derivatives of strain Δ*aeg1*(pJL03::mCherry-Aeg1) expressing GFP fusion of each of the divisome proteins from the P_{TAC} promoter grown in medium with ara were processed for imaging. The red arrows representative examples of the inability of fusion proteins to target to the septal ring. Bar, 5 µm. Images are representative of three parallel cultures.

B-D. A few dominant active mutants of FtsB and FtsW bypassed the need of Aeg1 by *A. baumannii.* Mutant $FtsB_{E65A}$ **(B)**, $FtsB_{D68H}$ **(B)**, $FtsL_{Q70K}$ **(C)**, $FtsW_{M254I}$ **(D)**, or $FtsW_{S274G}$ **(D)** was expressed from the IPTG-inducible promoter P_{TAC} in strain Δ*aeg1*(pJL03::Aeg1). Serially diluted cells were spotted onto LB agar containing ara or IPTG. Images were acquired after incubation at 37°C for 18 h **(B-D)**. Similar results were obtained in three independent experiments. The expression of the protein was probed with the HA-specific antibody after IPTG induction **(B-D)**. ICDH was probed as a loading control.

Fig. 6 A model for the function of Aeg1 in cell division of *A. baumannii*. In the early stages of Z-ring assembly, anchor proteins FtsA and ZipA tether FtsZ to the inner face of the plasma membrane. In the initial phase of cell division, a small amount of FtsN is recruited to the divisome in a FtsA-dependent manner **(left, recruitment phase)** (65). The Aeg1-ZipA-FtsN complex acts as a dynamic scaffold for recruiting downstream of Fts proteins. Once more FtsN is recruited to the divisome, it will activate both FtsA and the FtsQLB complex, which in turn activates FtsI in the periplasm (40). Note that constitutively active form of FtsA (FtsA*) acts on FtsW in the cytoplasm (37) so did the hyperactive mutants $FtsA_{E202K}$. These mutants all bypassed the need of Aeg1 **(right, activation phase)**. Constitutively active mutants were indicated by a star. The red arrows next to $FtsA_{E202K}$ or $FtsB_{E65A}$ indicate overexpression of these mutants.

Fig. 1-figure supplement 1 *aeg1* is essential for *A. baumannii* growth in the VBS medium. Strains were tested for growth by spotting serially diluted cells on medium with or without 1% arabinose. Images were acquired after incubation at 37°C for 18 h. Similar results were obtained in at least three independent experiments.

Fig. 1-figure supplement 2 Alignment of Aeg1 homologs from a few Gram-negative bacteria. Aeg1 of *A. baumannii* and its homologs from a member of the *Moraxellaceae* family, *E. coli* (strain s_6558), *Klebsiella pneumoniae* (strain 4300STDY7045912), and *Salmonella*

enterica (strain 350627) were compared with Jalview. Homology from high to low was presented in dark red, orange, yellow, light yellow, or no highlight.

Fig. 3-figure supplement 1 Alignment of FtsA proteins between *A. baumannii* and *E. coli*. The FtsA proteins from *A. baumannii* and *E. coli* were compared using Jalview. The residues highlighted by blue boxes indicate the site of dominant active sites in *E. coli* proteins, and corresponding mutations were made in their *A. baumannii* counterparts.

Fig. 4-figure supplement 1 GFP and mCherry fusion proteins rescued the growth defects of their corresponding mutants. *zipA*, *ftsB*, *ftsL*, and *ftsN* are essential cell division genes which were deleted by the method described in Figure 1A. The resulting bacterial strains were tested for growth by spotting serially diluted cells on medium with 1% arabinose or 0.5 mM IPTG (A). Strain Δ*aeg1*(P_{BAD}::mCherry-Aeg1) expressing mCherry fusion of Aeg1 from the P_{BAD} promoter grown in medium with or without ara were processed for imaging **(B)**. Images were acquired after incubation at 37°C for 18 h. Similar results were obtained in at least three independent experiments.

Fig. 5-figure supplement 1 Δ*aeg1*(P_{BAD}::mCherry) strain unable to exhibit expression of Aeg1-mCherry after 6 h period without ara. Cells of derivatives of strain Δ*aeg1*(P_{BAD}::mCherry-Aeg1) expressing mCherry fusion of Aeg1 from the P_{BAD} promoter grown in medium with ara were processed for imaging. Bar, 10 µm. Images are representative of three parallel cultures.

Fig. 5-figure supplement 2 Alignment of Fts proteins between *A. baumannii* and *E. coli*. The FtsB, FtsL, FtsW, and FtsI proteins from *A. baumannii* and *E. coli* were compared using Jalview. The residues highlighted by blue boxes indicate the site of dominant active sites in *E. coli* proteins, and corresponding mutations were made in their *A. baumannii* counterparts.

Figure 1-source data 1 Examining Aeg1 and Aeg1$^{\Delta N}$ expression through HA-specific antibody immunoblotting.

Figure 3-source data 1 Examining Aeg1, FtsA, FtsA$_{E202K}$, FtsA$_{D124A}$, FtsA$_{V144A}$, and FtsA$_{Q285A}$ expression through HA-specific antibody immunoblotting.

Figure 5-source data 1 Examining Aeg1, FtsB$_{E65A}$, FtsB$_{D68H}$, FtsL$_{Q70K}$, FtsW$_{M254I}$, and FtsW$_{S274G}$ expression through HA-specific antibody immunoblotting.

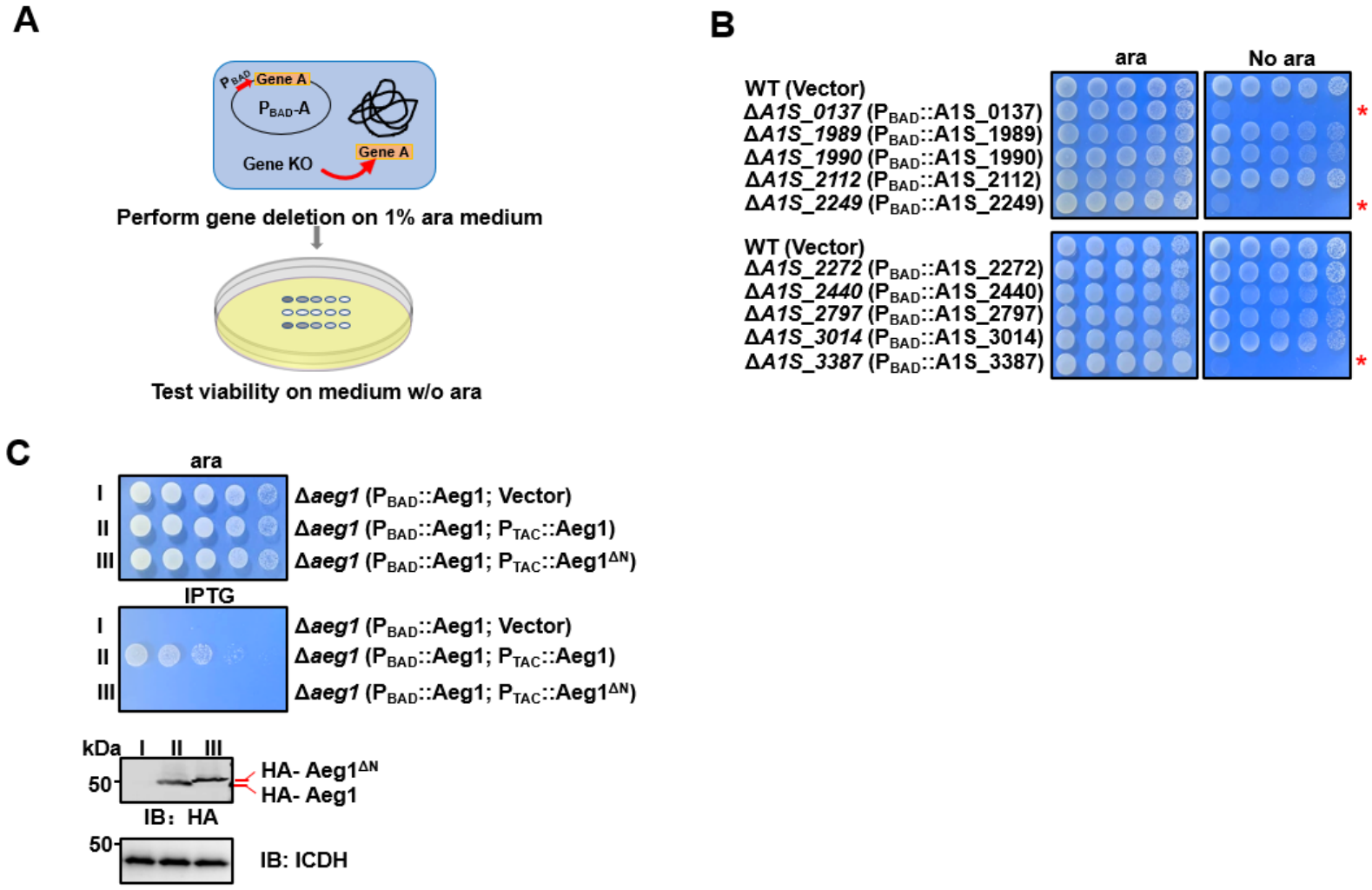
A
PBAD
Gene A
PBAD-A
Gene KO
Gene A
Perform gene deletion on 1% ara medium
Test viability on medium w/o ara
B
ara
No ara
WT (Vector)
ΔA1S_0137 (PBAD::A1S_0137)
ΔA1S_1989 (PBAD::A1S_1989)
ΔA1S_1990 (PBAD::A1S_1990)
ΔA1S_2112 (PBAD::A1S_2112)
ΔA1S_2249 (PBAD::A1S_2249)
*
*
WT (Vector)
ΔA1S_2272 (PBAD::A1S_2272)
ΔA1S_2440 (PBAD::A1S_2440)
ΔA1S_2797 (PBAD::A1S_2797)
ΔA1S_3014 (PBAD::A1S_3014)
ΔA1S_3387 (PBAD::A1S_3387)
*
C
ara
I
II
III
Δaeg1 (PBAD::Aeg1; Vector)
Δaeg1 (PBAD::Aeg1; PTAC::Aeg1)
Δaeg1 (PBAD::Aeg1; PTAC::Aeg1ΔN)
IPTG
I
II
III
Δaeg1 (PBAD::Aeg1; Vector)
Δaeg1 (PBAD::Aeg1; PTAC::Aeg1)
Δaeg1 (PBAD::Aeg1; PTAC::Aeg1ΔN)
kDa I II III
50
HA- Aeg1ΔN
HA- Aeg1
IB：HA
50
IB: ICDH

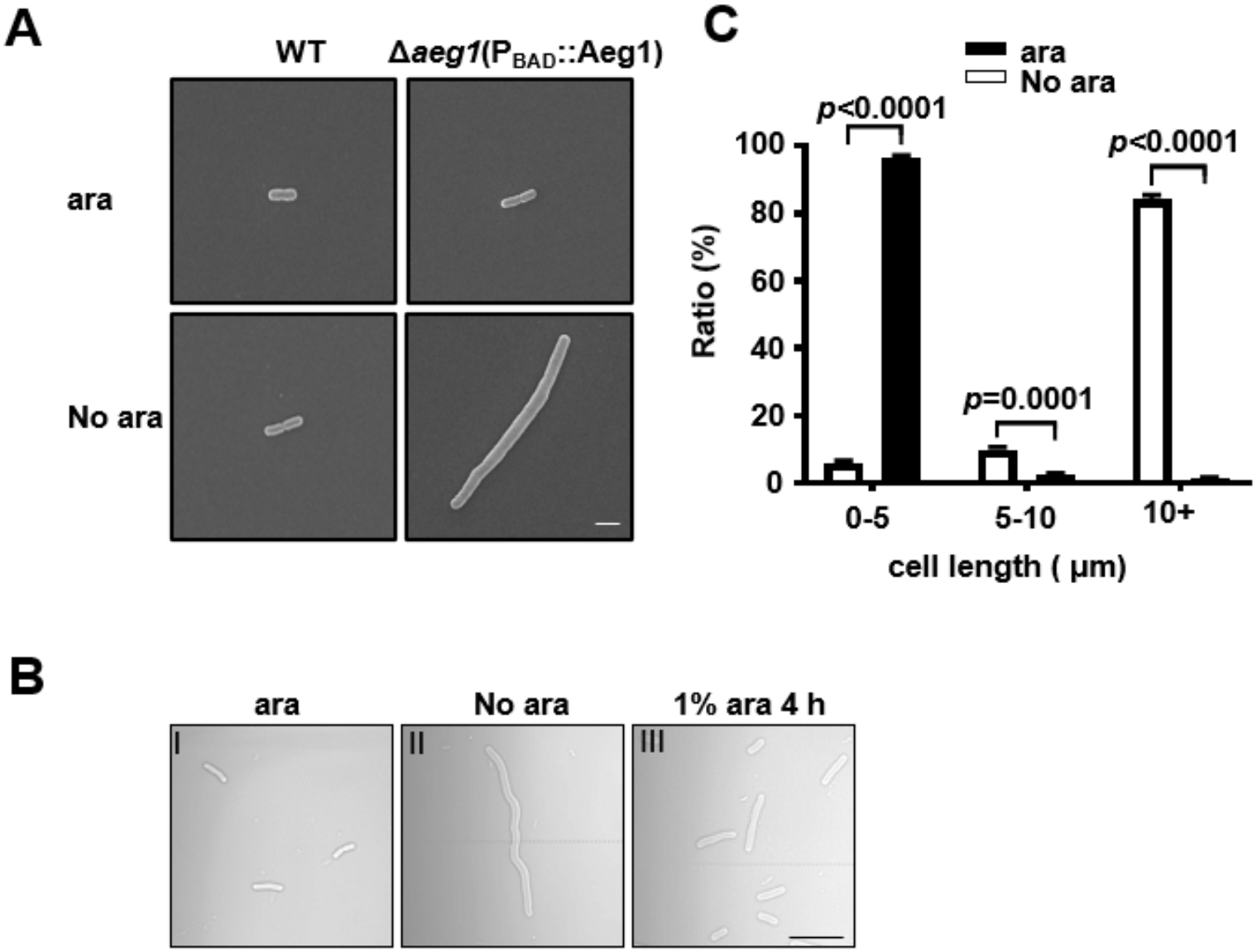
A
WT
Δaeg1(P_BAD::Aeg1)
ara
No ara
C
ara
No ara
p<0.0001
p<0.0001
p=0.0001
Ratio (%)
100
80
60
40
20
0
0-5
5-10
10+
cell length (μm)
B
ara
No ara
1% ara 4 h
I
II
III

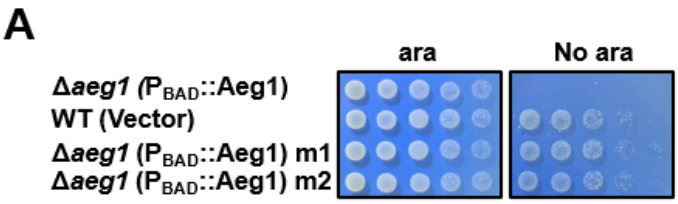
A
ara
No ara
Δaeg1 (PBAD::Aeg1)
WT (Vector)
Δaeg1 (PBAD::Aeg1) m1
Δaeg1 (PBAD::Aeg1) m2

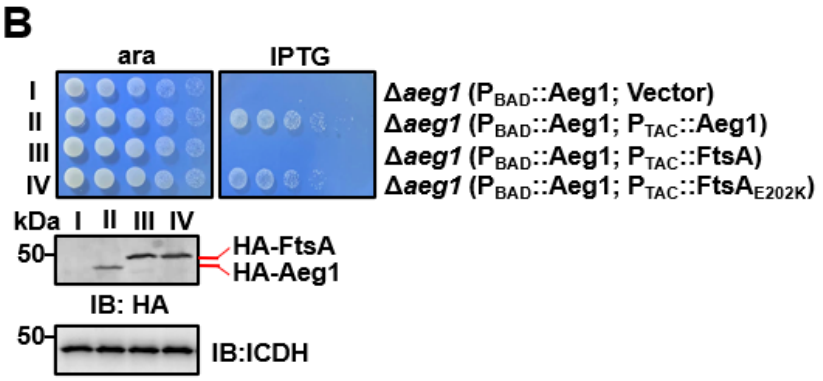
B
ara
IPTG
I
II
III
IV
Δaeg1 (PBAD::Aeg1; Vector)
Δaeg1 (PBAD::Aeg1; PTAC::Aeg1)
Δaeg1 (PBAD::Aeg1; PTAC::FtsA)
Δaeg1 (PBAD::Aeg1; PTAC::FtsAE202K)
kDa I II III IV
50
HA-FtsA
HA-Aeg1
IB: HA
50
IB:ICDH

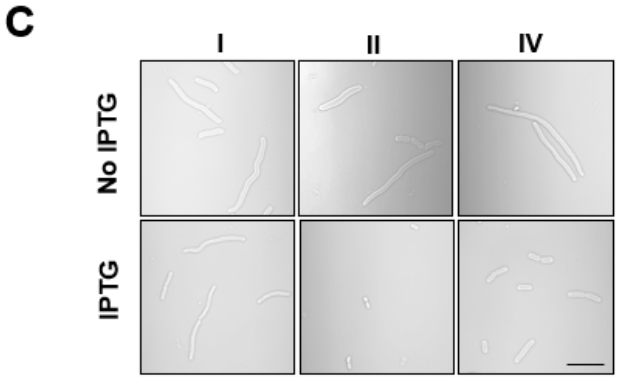
C
I
II
IV
No IPTG
IPTG

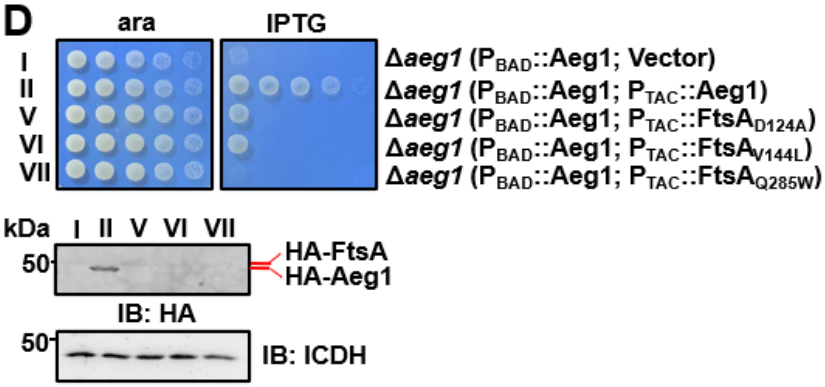
D
ara
IPTG
I
II
V
VI
VII
Δaeg1 (PBAD::Aeg1; Vector)
Δaeg1 (PBAD::Aeg1; PTAC::Aeg1)
Δaeg1 (PBAD::Aeg1; PTAC::FtsAD124A)
Δaeg1 (PBAD::Aeg1; PTAC::FtsAV144L)
Δaeg1 (PBAD::Aeg1; PTAC::FtsAQ285W)
kDa I II V VI VII
50
HA-FtsA
HA-Aeg1
IB: HA
50
IB: ICDH

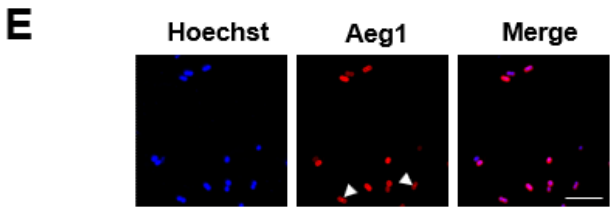
E
Hoechst
Aeg1
Merge

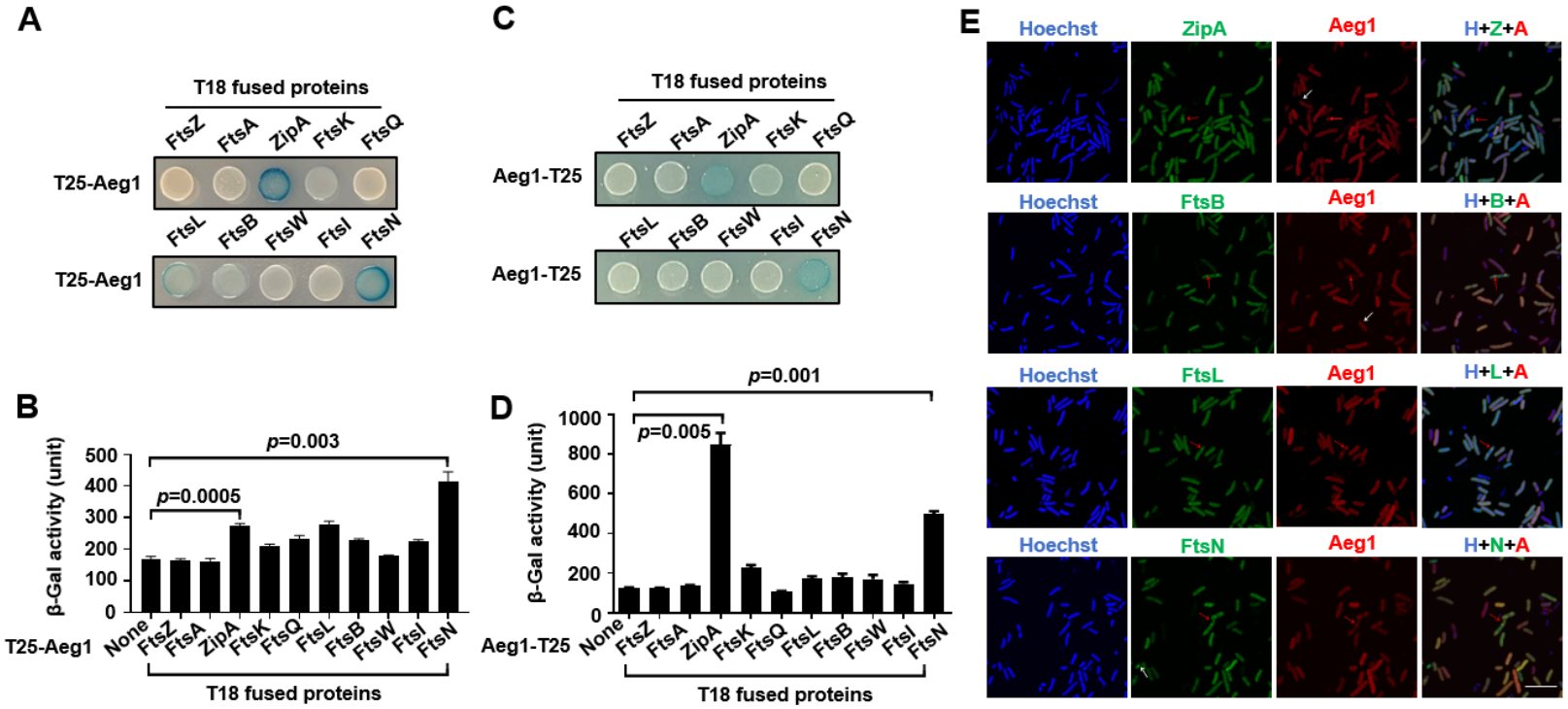
A
T18 fused proteins
FtsZ
FtsA
ZipA
FtsK
FtsQ
T25-Aeg1
FtsL
FtsB
FtsW
FtsI
FtsN
T25-Aeg1
C
T18 fused proteins
FtsZ
FtsA
ZipA
FtsK
FtsQ
Aeg1-T25
FtsL
FtsB
FtsW
FtsI
FtsN
Aeg1-T25
B
β-Gal activity (unit)
500
400
300
200
100
0
p=0.003
p=0.0005
T25-Aeg1
None
FtsZ
FtsA
ZipA
FtsK
FtsQ
FtsL
FtsB
FtsW
FtsI
FtsN
T18 fused proteins
D
β-Gal activity (unit)
1000
800
600
400
200
0
p=0.001
p=0.005
Aeg1-T25
None
FtsZ
FtsA
ZipA
FtsK
FtsQ
FtsL
FtsB
FtsW
FtsI
FtsN
T18 fused proteins
E
Hoechst
ZipA
Aeg1
H+Z+A
Hoechst
FtsB
Aeg1
H+B+A
Hoechst
FtsL
Aeg1
H+L+A
Hoechst
FtsN
Aeg1
H+N+A

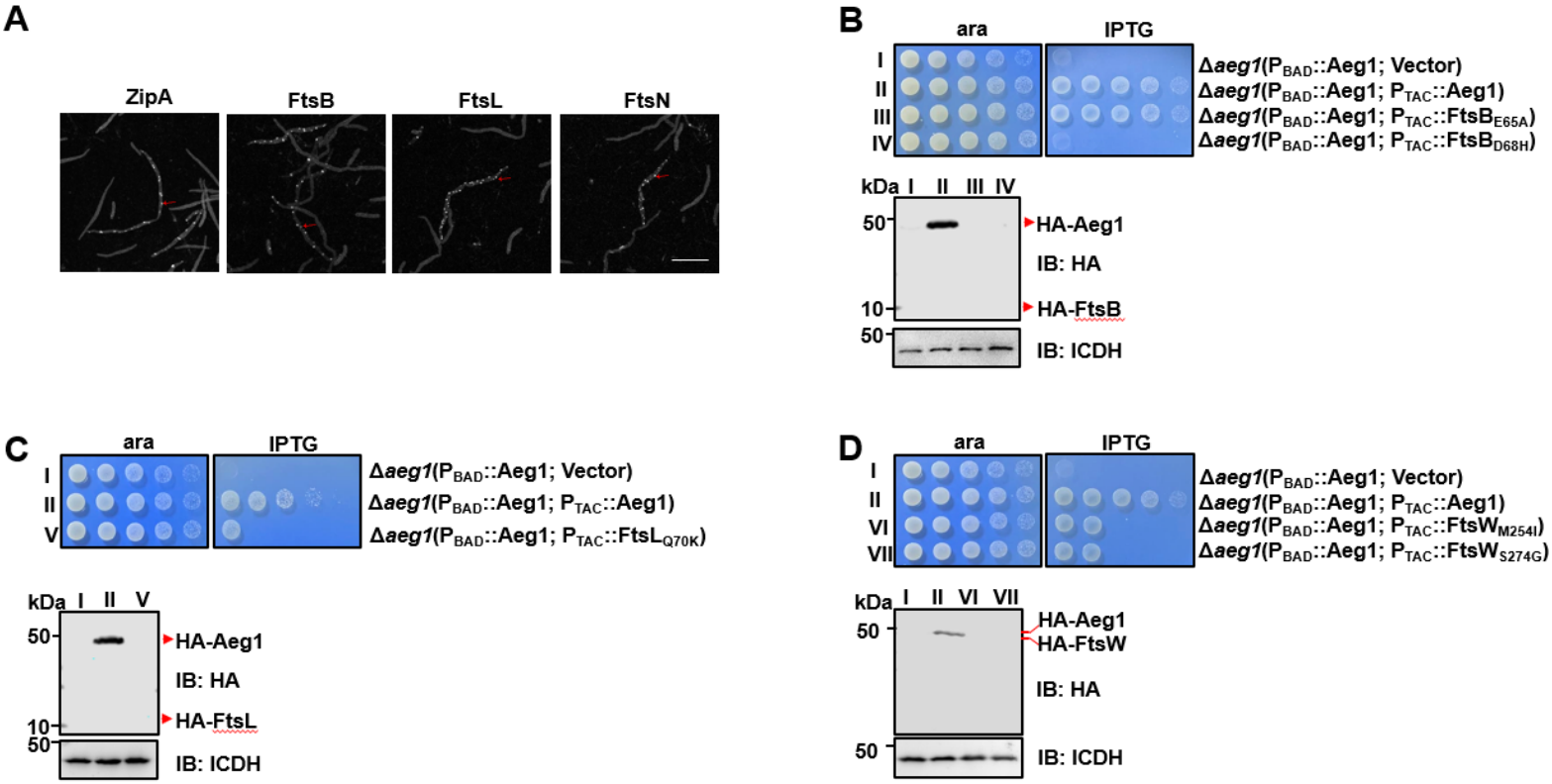
A
ZipA
FtsB
FtsL
FtsN
B
ara
IPTG
I
II
III
IV
Δaeg1(PBAD::Aeg1; Vector)
Δaeg1(PBAD::Aeg1; PTAC::Aeg1)
Δaeg1(PBAD::Aeg1; PTAC::FtsBE65A)
Δaeg1(PBAD::Aeg1; PTAC::FtsBD68H)
kDa I II III IV
50
HA-Aeg1
IB: HA
10
HA-FtsB
50
IB: ICDH
C
ara
IPTG
I
II
V
Δaeg1(PBAD::Aeg1; Vector)
Δaeg1(PBAD::Aeg1; PTAC::Aeg1)
Δaeg1(PBAD::Aeg1; PTAC::FtsLQ70K)
kDa I II V
50
HA-Aeg1
IB: HA
10
HA-FtsL
50
IB: ICDH
D
ara
IPTG
I
II
VI
VII
Δaeg1(PBAD::Aeg1; Vector)
Δaeg1(PBAD::Aeg1; PTAC::Aeg1)
Δaeg1(PBAD::Aeg1; PTAC::FtsWM254I)
Δaeg1(PBAD::Aeg1; PTAC::FtsWS274G)
kDa I II VI VII
50
HA-Aeg1
HA-FtsW
IB: HA
50
IB: ICDH

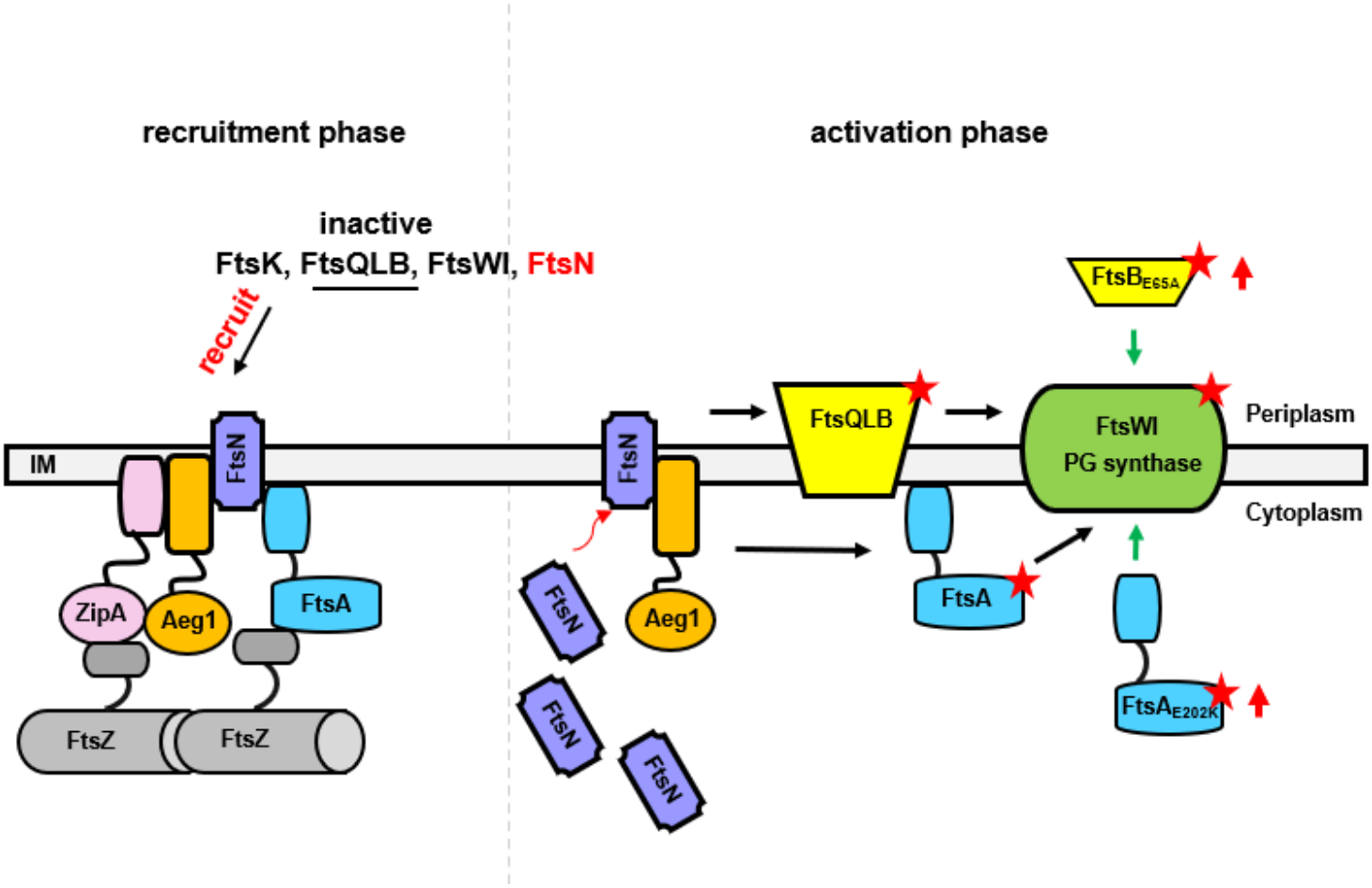
recruitment phase
activation phase
inactive
FtsK, FtsQLB, FtsWI, FtsN
recruit
IM
FtsN
ZipA
Aeg1
FtsA
FtsZ
FtsZ
FtsN
Aeg1
FtsN
FtsN
FtsN
FtsQLB
FtsA
FtsB$_{E65A}$
FtsWI
PG synthase
Periplasm
Cytoplasm
FtsA$_{E202K}$

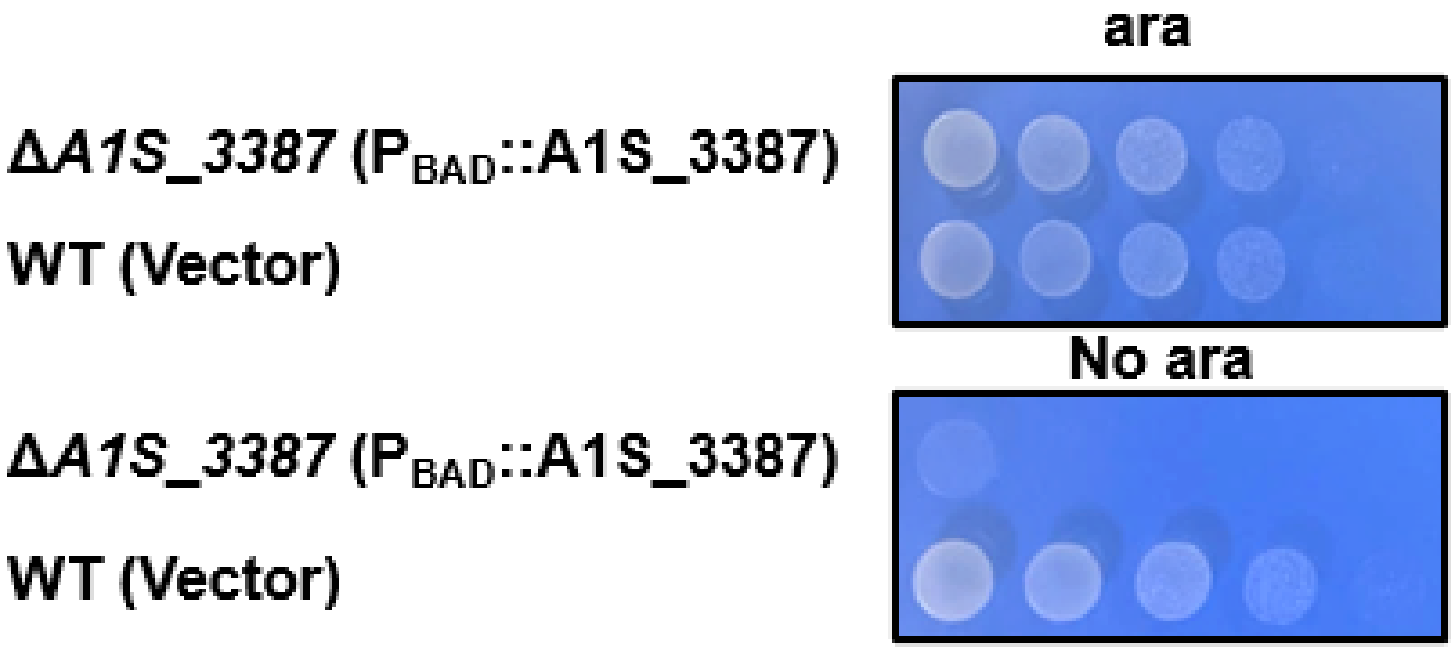
ara
Δ*A1S_3387* (P_{BAD}::A1S_3387)
WT (Vector)
No ara
Δ*A1S_3387* (P_{BAD}::A1S_3387)
WT (Vector)

```
Acinetobacter baumannii  (ATCC 17978)          1 ------MIAPRQGLFASLLIISFALHTFLLVIATTHQLNENRASQGQLMTSQLVAD  50
Klebsiella pneumoniae (4300STDY7045912)        1 ------MIAPRQGLFASLLIISFALHTFLLVIATTHQLNENRASQGQLMTSQLVAD  50
Escherichia coli (s_6558)                      1 ------MIAPRQGLFASLLIISFALHTFLLVIATTHQLNENRASQGQLMTSQLVAD  50
Moraxellaceae bacterium                        1 ------MNAPRQGLFASLLIVSFALHTFLLVIATTHQLNENRASQGQLMTSQLVAD  50
Salmonella enterica (350627)                   1 MPWKFTLNAPRQGLFASLLIVSFALHTFLLVIATTHQLNENRASQGQLMTSQLVTD  56

Acinetobacter baumannii  (ATCC 17978)         51 SLSELEPANTVSLALIANRYATNPSVASIRILDANKQVLATSGMSKTRQGEIFVRD 106
Klebsiella pneumoniae (4300STDY7045912)       51 SLSELEPANTVSLALIANRYATNPSVASIRILDANKQVLATSGMSKTRQGEIFVRD 106
Escherichia coli (s_6558)                     51 SLSELEPANTVSLALIANRYATNPSVASIRILDANKQVLATSGMSKTRQGEIFVRD 106
Moraxellaceae bacterium                       51 SLSELEPANTVSLALVANRYATNPSIASIRILDANKQVLATSGMAKTRQGEIFVRD 106
Salmonella enterica (350627)                  57 SLTELEPANTVSLALLANRYATNPSVASIRILDANKQVLATSGMSQTRQGEVFVRD 112

Acinetobacter baumannii  (ATCC 17978)        107 ALQNEKKVGSIEITLIQPSIGEILRTQWLAILASLFLHVLLWLAYRAIARPTRSEY 162
Klebsiella pneumoniae (4300STDY7045912)      107 ALQNEKKVGSIEITLIQPSIGEILRTQWLAILASLFLHVLLWLAYRAIARPTRSEY 162
Escherichia coli (s_6558)                    107 ALQNEKKVGSIEITLIQPSIGEILRTQWLAILASLFLHVLLWLAYRAIARPTRSEY 162
Moraxellaceae bacterium                      107 ALQNEKKVGTVEITLIQPSIGEILRTQWLAILASLFIHGLIWLAYRAIARPTRSEY 162
Salmonella enterica (350627)                 113 ALQNEKKVGSIEITLIQPSIGEILRTQWLAILVSFLIHGLLWLAYRAIARPSRSEY 168

Acinetobacter baumannii  (ATCC 17978)        163 LARINEENRLKHEIQELTQALALEKQNTVTLVAQAQQQAKAKPIVRSQPEK-SLES 217
Klebsiella pneumoniae (4300STDY7045912)      163 LARINEENRLKHEIQELTQALALEKQNTVTLVAQAQQQAKAKPIVRSQPEK-SLES 217
Escherichia coli (s_6558)                    163 LARINEENRLKHEIQELTQALALEKQNTVTLVAQAQQQAKAKPIVRSQPEK-SLES 217
Moraxellaceae bacterium                      163 LARINQENHLKHEIQRLTQALALEKQNTVTLVAQAQQQAKAQPKSRIEKNSTDQAQ 218
Salmonella enterica (350627)                 169 LARINNESRLKHEIQQLTQALELEKQNTVTLIAQAKQQAKPKV--STVSETLEQDA 222

Acinetobacter baumannii  (ATCC 17978)        218 TDQNTLALNIQFYDPKQLLSSVNQSVSVPYFKLCQLFLNKSIELCTKHYHLKATDI 273
Klebsiella pneumoniae (4300STDY7045912)      218 TDQNTLALNIQFYDPKQLLSSVNQSVSVPYFKLCQLFLNKSIELCTKHYHLKATDI 273
Escherichia coli (s_6558)                    218 TDQNTLALNIQFYDPKQLLSSVNQSVSVPYFKLCQLFLNKSIELCTKHYHLKATDI 273
Moraxellaceae bacterium                      219 LDHQTVALNIQFYDPKQLLSSVNQSVSVPYFKLCQLFLDKSIDLCAKHYQLDVAQI 274
Salmonella enterica (350627)                 223 QADHTLALNIQFYDPKQLLNSVNQSVSVPYFKLCQIFLNKSIELCAKHYQLSPSTI 278

Acinetobacter baumannii  (ATCC 17978)        274 DVVDEFHAEGATLAISTSHPHAVECLLMVGTVFQLLSDVLYKRYREDKRFALQTRS 329
Klebsiella pneumoniae (4300STDY7045912)      274 DVVDEFHAEGATLAISTSHPHAVECLLMVGTVFQLLSDVLYKRYREDKRFALQTRS 329
Escherichia coli (s_6558)                    274 DVVDEFHAEGATLAISTSHPHAVECLLMVGTVFQLLSDVLYKRYREDKRFALQTRS 329
Moraxellaceae bacterium                      275 RVVQEFNAEGATLSTTSEHAHALECLMMVGAVFQLLADVLYKRYREDKRFALQTRG 330
Salmonella enterica (350627)                 279 NVIHEFNANGADLSISDQDAHAVECLLMIGSVFQLLSDVLYKRYREDKRFALQTRS 334

Acinetobacter baumannii  (ATCC 17978)        330 AVCNAVEAMQIDAKEAAQRLAQHLHAKESALYLDNEQLKAIQDSYQLVAMPNPSNV 385
Klebsiella pneumoniae (4300STDY7045912)      330 AVCNAVEAMQIDAKEAAQRLAQHLHAKESALYLDNEQLKAIQDSYQLVAMPNPSNV 385
Escherichia coli (s_6558)                    330 AVCNAVEAMQIDAKEAAQRLAQHLHAKES---------------------------- 358
Moraxellaceae bacterium                      331 AVASAVDAMQLDAIEAAKRLTQHLHAKEAALHLNHEQLKTVQNSYELVIMPNPSNI 386
Salmonella enterica (350627)                 335 ATSTAVTAMQLDAVQAAQRLTSHLHAKESALHLNNEQLKAISECYQLIAMPNPSSV 390

Acinetobacter baumannii  (ATCC 17978)        386 MTRHAFMINGMNAECAELAQNIRTEILMGKKSIPQNDSPSSAAS--           429
Klebsiella pneumoniae (4300STDY7045912)      386 MTRHAFMINGMNAECAELAQNIRTEILMGKKSIPQNDSPSSAAS--           429
Escherichia coli (s_6558)                    ------------------------------------------------
Moraxellaceae bacterium                      387 MTRHAFMINGMNEQCATLAQDLRTEILMGKKVKASTES-------           424
Salmonella enterica (350627)                 391 LTRHAFMQNGMNTECAEVAQQIRTEILMGKKAKASIENQTDPQSEA           436
```

FtsA

```
Acb     1 --MSEAVPSVVAIDIGTHKVSVLIGKIHAPDNIQVIGMATARNRGMNKGKIVSLDKVIAAIKNAVAEAENMA  70
E.coli  1 MIKATDRKLVVGLEIGTAKVAALVGEVLPDGMVNIIGVGSCPSRGMDKGGVNDLESVVKCVQRAIDQAELMA  72

Acb    71 ECRIHSAWVSIPSTELQSFYASGRTPVANPAHVITTNEVVRALELAKASHVTSDYYLASAVPLGFELGDSSE 142
E.coli 73 DCQISSVYLALSGKHISCQNEIGMVPISEEEV--TQEDVENVVHTAKSVRVRDEHRVLHVIPQEYAI-DYQE 141

Acb   143 WVQNPINMTAHSMTGHYQLMMMPIATMQNLDRAMKGANIGVEKMVVSCLATAEASLLKDEKEYGVCLVDIGA 214
E.coli 142 GIKNPVGLSGVRMQAKVHLITCHNDMAKNIVKAVERCGLKVDQLIFAGLASSYSVLTEDERELGVCVVDIGG 213

Acb   215 GITNLAVYLDGRLALARTLQRGGEHVTRDIAAVLQTTTEEAERIKILHGCVDLSAVKPDHMIQVQGID--GP 284
E.coli 214 GTMDIAVYTGGALRHTKVIPYAGNVVTSDIAYAFGTPPSDAEAIKVRHGCALGSIVGKDESVEVPSVGGRPP 285

Acb   285 QTISRIELAEIIIARYEEIFSQ-------IREELEQSGAIHGLYHGVVLTGDACQIEGMVSLARRMLGVSAH 349
E.coli 286 RSLQRQTLAEVIEPRYTELLNLVNEEILQLQEKLRQQGVKHHLAAGIVLTGGAAQIEGLAACAQRVFHTQVR 357

Acb   350 LGNPPLQVYADDQHQAALRRSMYATAAGLLMFSQSELQEAVEEP--EEGNDRSVWERMVNGWNAFNSKLKAI 419
E.coli 358 IGAPLNITGLTD----YAQEPYYSTAVGLLHYGKESHLNGEAEVEKRVTASVGSWIKRLNSWLRKEF----- 420
Acb
           420 F                                                                     420
               -
```

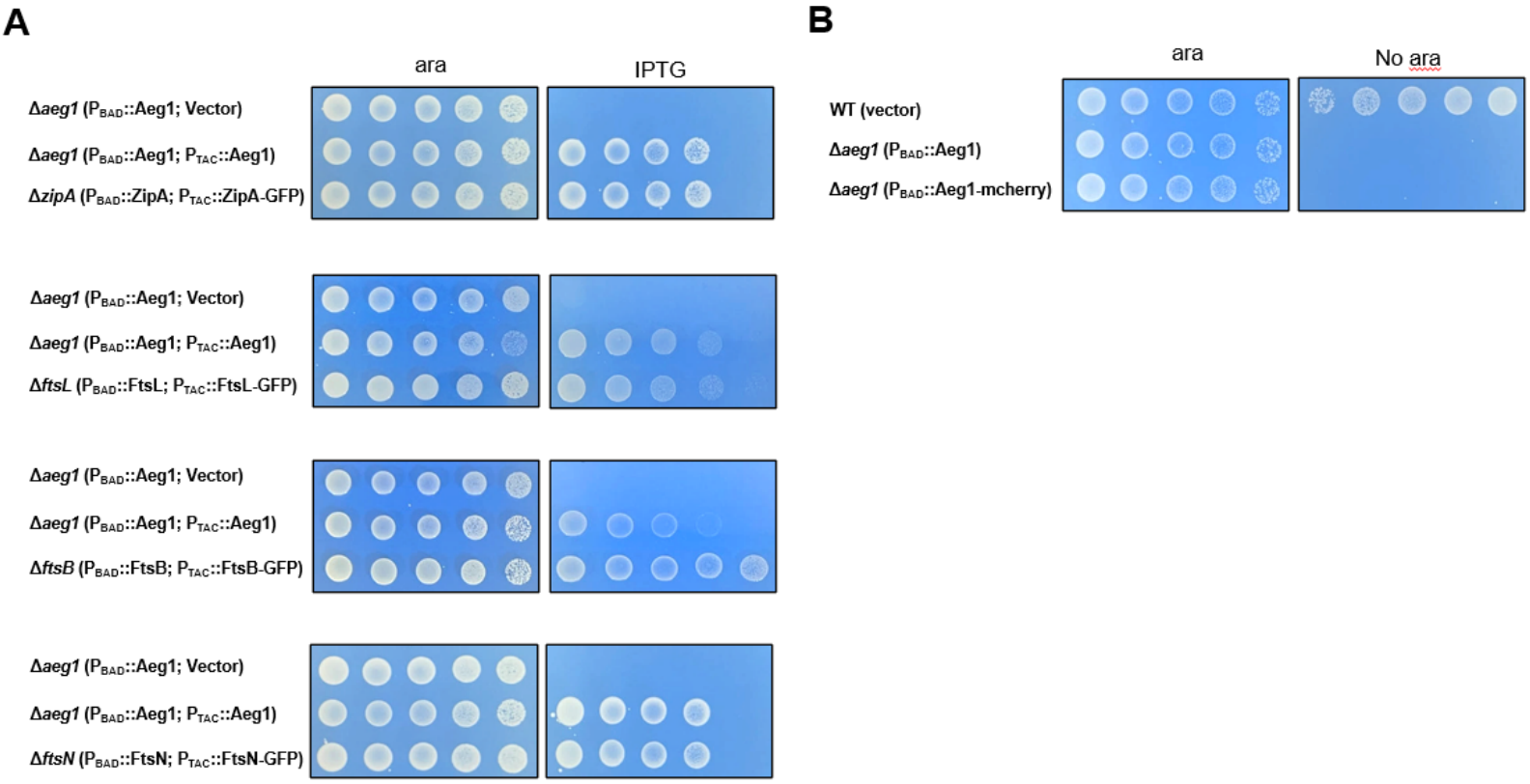
A
ara
IPTG
Δaeg1 (PBAD::Aeg1; Vector)
Δaeg1 (PBAD::Aeg1; PTAC::Aeg1)
ΔzipA (PBAD::ZipA; PTAC::ZipA-GFP)
Δaeg1 (PBAD::Aeg1; Vector)
Δaeg1 (PBAD::Aeg1; PTAC::Aeg1)
ΔftsL (PBAD::FtsL; PTAC::FtsL-GFP)
Δaeg1 (PBAD::Aeg1; Vector)
Δaeg1 (PBAD::Aeg1; PTAC::Aeg1)
ΔftsB (PBAD::FtsB; PTAC::FtsB-GFP)
Δaeg1 (PBAD::Aeg1; Vector)
Δaeg1 (PBAD::Aeg1; PTAC::Aeg1)
ΔftsN (PBAD::FtsN; PTAC::FtsN-GFP)
B
ara
No ara
WT (vector)
Δaeg1 (PBAD::Aeg1)
Δaeg1 (PBAD::Aeg1-mcherry)

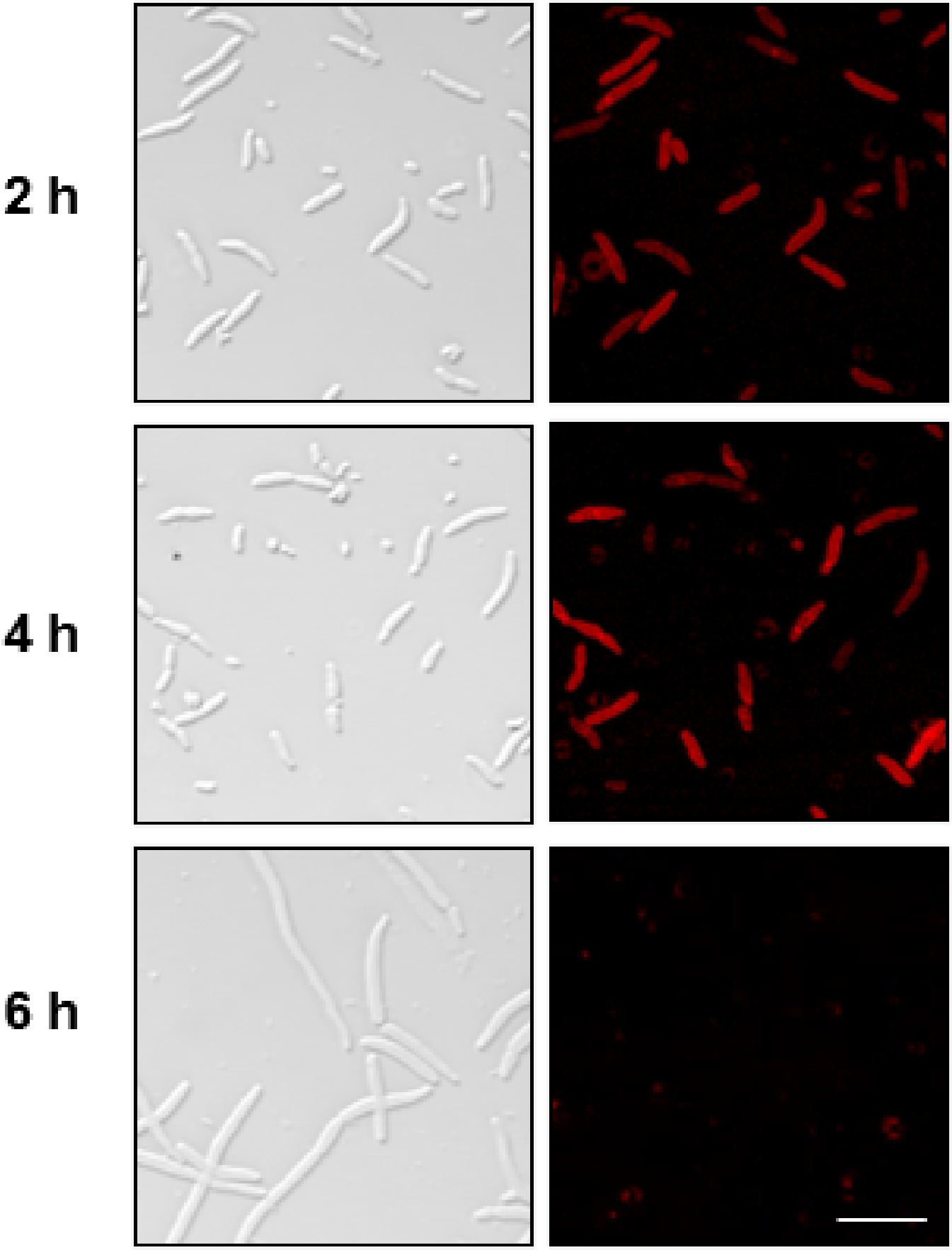
2 h
4 h
6 h

FtsB

FtsL

FtsI

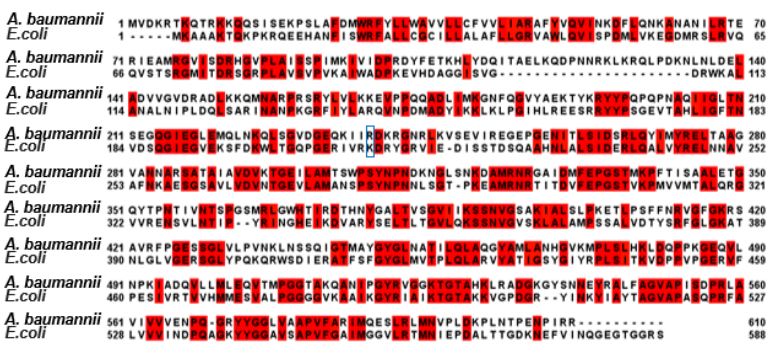

FtsW